DPD, and OPRT), the OPRT pathway was the most important for activating 5-FU. Hence, the ratio of OPRT and DPD was also evaluated in this study. The OPRT/DPD ratio was significantly higher in responding tumors than in nonresponding ones, and patients with tumors with a high OPRT/DPD ratio survived longer than those with tumors with a low OPRT/DPD ratio. Therefore, further studies are necessary to evaluate whether the OPRT/DPD ratio could be adopted as a possible predictor of the effectiveness of other fluoropyrimidine analogues.

In conclusion, using the TP/DPD ratio as a prognostic parameter for pancreatic cancer may help select patients for more intensive surgical approaches. However, the conclusions have been drawn from a retrospective study of a small number of patients. Moreover, since the time that these patients were treated, various advances have occurred, not only in surgical procedures but also in adjuvant therapies for pancreatic cancer. Further study is needed to investigate the relationship between TP and OPRT mRNA expression (and the ratio of these expressions to DPD mRNA expression) and features such as prognosis and the antitumor effect of fluoropyrimidine-based chemotherapy in pancreatic cancer.

Acknowledgments This study was supported by part of The Board for Cancer Research Project, a cooperative project of TAIHO Pharmaceutical Co., Ltd and The University of Tokushima.

References

1. Heggie GD, Sommadossi JP, Cross DS, et al. (1987) Clinical pharmacokinetics of 5-fluorouracil and its metabolites in plasma, urine, and bile. Cancer Res 47:2203–2206
2. Pinedo HM, Peters GJ (1988) 5-Fluorouracil: biochemistry and pharmacology. J Clin Oncol 6:1653–1664
3. Santi DV, McHenry CS, Sommer H (1974) Mechanisms of interaction of thymidylate synthase with 5-fluorodeoxyuridine. Biochemistry 13:471–480
4. Miyazono K, Okabe T, Urabe A, et al. (1987) Purification and properties of an endothelial cell growth factor from human platelets. J Biol Chem 262:4098–4103
5. Ishikawa F, Miyazono K, Hellman U, et al. (1989) Identification of angiogenic activity and the cloning and expression of platelet-derived endothelial cell growth factor. Nature 338:556–562
6. Sumizawa T, Furukawa T, Haraguchi M, et al. (1993) Thymidine phosphorylase activity associated with platelet-derived endothelial cell growth factor. J Biochem 114:9–14
7. Haraguchi M, KMiyadera K, Uemura K, et al. (1994) Angiogenic activity of enzymes. Nature 368:198
8. Miyadera K, Sumizawa T, Haraguchi M, et al. (1995) Role of thymidine phosphorylase activity in the angiogenic effect of platelet-derived endothelial cell growth factor/thymidine phosphorylase. Cancer Res 55:1687–1690
9. Miwa M, Cook A, Ishitsuka H. (1986) Enzymatic cleavage of various fluorinated pyrimidine nucleosides to 5-fluorouracil and their antiproliferative activities in human and murine tumor cells. Chem Pharm Bull 34:4225–4232
10. Ishitsuka H. (2000) Capecitabine: preclinical pharmacology studies. Invest New Drugs 18:343–354
11. Shirasaka T, Shimamoto Y, Fukushima M. (1993) Inhibition by oxonic acid of gastrointestinal toxicity of 5-fluorouracil without loss of its antitumor activity in rats. Cancer Res 53:4004–4009
12. Inaba M, Mitsuhashi J, Sawada H, et al. (1996) Reduced activity of anabolizing enzymes in 5-fluorouracil-resistant human stomach cancer cells. Jpn J Cancer Res 87:212–220
13. Kanai F, Kawakami T, Hamada H, et al. (1998) Adenovirus-mediated transduction of *Escherichia coli* uracil phosphoribosyltransferase gene sensitizes cancer cells to low concentrations of 5-fluorouracil. Cancer Res 58:1946–1951
14. Inaba M, Sawada H, Sadata A, et al. (1999) Circumvention of 5-fluorouracil resistance in human stomach cancer cells by uracil phosphoribosyltransferase gene transduction. Jpn J Cancer Res 90: 349–354
15. Salonga D, Danenberg KD, Johnson M, et al. (2000) Colorectal tumors responding to 5-fluorouracil have low gene expression levels of dehydropyrimidine dehydrogenase, thymidylate synthase, and thymidine phosphorylase. Clin Cancer Res 6:1322–1327
16. Ishikawa Y, Kubota T, Otani Y, et al. (2000) Dihydropyrimidine dehydrogenase and messenger RNA levels in gastric cancer: possible predictor for sensitivity to 5-fluorouracil. Jpn J Cancer Res 91:105–112
17. Etienne MC, Cheradame S, Fischel JL, et al. (1995) Response to fluorouracil therapy in cancer patients: the role of tumoral dihydropyrimidine dehydrogenase activity. J Clin Oncol 13:1663–1670
18. Ishikawa T, Sekiguchi F, Fukase Y, et al. (1998) Positive correlation between the efficacy of capecitabine and doxifluridine and the ratio of thymidine phosphorylase to dihydropyrimidine dehydrogenase activities in tumors in human cancer xenografts. Cancer Res 58:685–690
19. Terashima M, Fujiwara H, Takagane A, et al. (2002) Role of thymidine phosphorylase and dihydropyrimidine dehydrogenase in tumour progression and sensitivity to doxifluridine in gastric cancer patients. Eur J Cancer 38:2375–2381
20. Ichikawa W, Uetake H, Shirota Y, et al. (2003) Both gene expression for orotate phosphoribosyltransferase and its ratio to dihydropyrimidine dehydrogenase influence outcome following fluoropyrimidine-based chemotherapy for metastatic colorectal cancer. Br J Cancer 89:1486–1492
21. Japan Pancreas Society (2003) Classification of pancreatic carcinoma, Second English edition. Kanehara, Tokyo
22. Gibson UE, Heid CA, Williams PM. (1996) A novel method for real time quantitative RT-PCR. Genome Res 6:995–1001
23. Ichikawa W, Takahashi T, Suto K, et al. (2004) Thymidylate synthase and dihydropyrimidine dehydrogenase gene expression in relation to differentiation of gastric cancer. Int J Cancer 112: 967–973
24. Kamoshida S, Matsuoka H, Shiogama K, et al. (2004) Immunohistochemical analysis of thymidylate synthase, $p16^{INK4a}$, cyclin-dependent kinase 4 and cyclin D1 in colorectal cancers receiving preoperative chemotherapy: significance of $p16^{INK4a}$ mediated cellular arrest as an indicator of chemosensitivity to 5-fluorouracil. Pathol Int 54:564–575
25. Kamoshida S, Matsuoka H, Shiogama K, et al. (2004) Immunohistochemical evaluation of thymidylate synthase (TS) and $p16^{INK4}$ in advanced colorectal cancer: implication of TS expression in 5-FU-based adjuvant chemotherapy. Jpn J Clin Oncol 34:594–601
26. Konno S, Takebayashi Y, Aiba M, et al. (2001) Clinicopathological and prognostic significance of thymidine phosphorylase and proliferating cell nuclear antigen in gastric carcinoma. Cancer Lett 166:103–111
27. Nishimura G, Terada I, Kobayashi T, et al. (2002) Thymidine phosphorylase and dihydropyrimidine dehydrogenase levels in primary colorectal cancer show a relationship to clinical effects of 5′-deoxy-5-fluorouridine as adjuvant chemotherapy. Oncol Rep 9:479–482
28. Mori K, Hasegawa M, Nishida M, et al. (2000) Expression levels of thymidine phosphorylase and dihydropyrimidine dehydrogenase in various human tumor tissues. Int J Oncol 17:33–38
29. Fujioka S, Yoshida K, Yanagisawa S, et al. (2001)Angiogenesis in pancreatic carcinoma. Cancer 92:1788–1797
30. Mizutani Y, Wada H, Fukushima M, et al. (2004) Prognostic significance of orotate phosphoribosyltransferase activity in bladder carcinoma. Cancer 100:723–731
31. Diasio RB, Lu Z (1994) Dihydropyrimidine dehydrogenase activity and fluorouracil chemotherapy. J Clin Oncol 12:2239–2242
32. Etienne MC, Cheradame S, Fischel JL, et al. (1995) Response to fluorouracil therapy in cancer patients: the role of tumoral

dihydropyrimidine dehydrogenase activity. J Clin Oncol 13: 1663–1670
33. Nita ME, Tominaga O, Nagawa H, et al. (1998) Dihydropyrimidine dehydrogenase but not thymidylate synthase expression is associated with resistance to 5-fluorouracil in colorectal cancer. Hepatogastroenterology 45:2117–2122
34. Hiroyasu S, Shiraishi M, Samura H, et al. (2001) Clinical relevance of the concentrations of both pyrimidine nucleoside phosphorylase (PyNPase) and dihydropyrimidine dehydrogenase (DPD) in colorectal cancer. Jpn J Clin Oncol 31:65–68
35. Fujiwaki R, Hata K, Nakayama K, et al. (2000) Gene expression for dihydropyrimidine dehydrogenase and thymidine phosphorylase influences outcome in epithelial ovarian cancer. J Clin Oncol 18:3946–3951
36. Kohne CH, Peters GJ. (2000) UFT: mechanism of drug action. Oncology 14:13–18

Modern Pathology (2007) 20, 552–561
© 2007 USCAP, Inc All rights reserved 0893-3952/07 $30.00
www.modernpathology.org

Fascin overexpression in intraductal papillary mucinous neoplasms (adenomas, borderline neoplasms, and carcinomas) of the pancreas, correlated with increased histological grade

Hiroshi Yamaguchi[1], Takahiro Inoue[1], Takashi Eguchi[1,4], Yoshihiro Miyasaka[1], Kenoki Ohuchida[2], Kazuhiro Mizumoto[2], Tomomi Yamada[3], Koji Yamaguchi[2], Masao Tanaka[2] and Masazumi Tsuneyoshi[1]

[1]*Department of Anatomic Pathology, Graduate School of Medical Sciences, Kyushu University, Fukuoka, Japan;* [2]*Department of Surgery and Oncology, Graduate School of Medical Sciences, Kyushu University, Fukuoka, Japan;* [3]*Department of Medical Information Science, Kyushu University Hospital, Fukuoka, Japan and* [4]*Department of Pathology, Iizuka Hospital, Iizuka, Japan*

Intraductal papillary mucinous neoplasm (IPMN) is a well-established entity in pancreatic neoplasms and a precursor of infiltrating adenocarcinoma. Fascin, an actin-bundling protein involved in cellular motility, is upregulated in many human neoplasms. Its overexpression in pancreatic intraepithelial neoplasia, a precancerous lesion sharing many characteristics with IPMN, has been reported. However, fascin expression in IPMN remains unknown. The aim of this study was to investigate fascin expression in IPMNs and to elucidate its relationship to clinicopathological features, including histological grade and phenotypic subclassification. We evaluated fascin expression by immunohistochemistry in 116 surgical specimens, followed by quantitative analysis of fascin mRNA expression using a laser microdissection system and real-time reverse-transcriptase polymerase chain reaction in eight frozen samples. Fascin expression was significantly higher in borderline neoplasms (25/29, 86%) and carcinomas (37/42, 88%) than in adenomas (23/45, 51%) ($P<0.05$, respectively), but no difference was observed between borderline neoplasms and carcinomas. With regard to the subclassification, intestinal-type neoplasms (35/39, 90%) were more frequently positive for fascin than gastric-type neoplasms (36/59, 61%) ($P<0.05$). Two oncocytic-type neoplasms were both fascin-negative. Fascin mRNA expression seemed to be higher in moderately to severely dysplastic epithelium than in mildly dysplastic epithelium (not statistically significant), supporting the immunohistochemical experiments. Our findings suggest that fascin overexpression is involved in the progression of IPMN. Fascin could become a new therapeutic target for inhibition of their progression.
Modern Pathology (2007) **20,** 552–561. doi:10.1038/modpathol.3800763; published online 30 March 2007

Keywords: intraductal papillary mucinous neoplasm; fascin; immunohistochemistry; laser microdissection; real-time RT-PCR; phenotypic subclassification

Intraductal papillary mucinous neoplasm (IPMN) is a well-established entity in pancreatic neoplasms. It was first reported in 1982 as a special type of pancreatic neoplasm with a characteristic endoscopic finding of extrusion of mucin through the ampulla of Vater.[1] At present, the term is used to unify tumors characterized by intraductal proliferation of neoplastic mucinous epithelium, which usually forms papillae and leads to cystic dilation of the pancreatic ducts.[2,3] Because IPMNs show a broad spectrum of dysplasia ranging from adenoma and borderline neoplasm to carcinoma *in situ*, the existence of an adenoma–carcinoma sequence is probable. In addition, some IPMNs are associated with infiltrating adenocarcinoma. Therefore, IPMN is gaining attention as a precursor of infiltrating adenocarcinoma in the pancreas as well as pancreatic intraepithelial neoplasia (PanIN).[4–6] Investigation of factors correlated with the progression of noninvasive and/or invasive IPMNs is important.

Correspondence: Dr H Yamaguchi, MD, Department of Anatomic Pathology, Pathological Sciences, Graduate School of Medical Sciences, Kyushu University, 3-1-1 Maidashi, Higashi-ku, Fukuoka, 812-8582, Japan.
E-mail: h-yama@surgpath.med.kyushu-u.ac.jp
Received 20 October 2006; revised 17 January 2007; accepted 18 January 2007; published online 30 March 2007

Several authors have proposed subclassification systems for IPMN based on histological phenotypes and/or immunohistochemical profiles of mucin core protein (MUC) expression.[7–13] Recently, a consensus on the subclassification of IPMNs was agreed among international experts on pancreatic precursor lesions, and published.[14] Subclassification makes it easier to compare studies among different institutions and understand the biological behavior, and is essential for future studies of IPMN.

Fascin-1 (also known as fascin) is a globular actin cross-linking protein. It is required for the formation of actin-based cell-surface protrusions that are essential for cellular migration and cell–matrix adhesion.[15–17] In normal epithelial cells, fascin expression is usually absent or very low, but it is significantly upregulated in transformed epithelial cells and several types of human carcinoma such as lung,[18,19] breast,[20–23] esophagus,[24,25] stomach,[26] colon,[27] pancreas,[28–31] biliary tract and ampulla,[31,32] ovary,[33] urinary bladder,[34] and skin.[35] Among the above neoplasms, fascin upregulation is most frequently observed in pancreatic infiltrating adenocarcinoma.[28,30,31] It is interesting that PanIN shows fascin expression despite being an intraepithelial neoplasia.[29,30] In general, in tumors of other organs, expression of fascin is especially strong in areas of infiltration, or is limited to such areas. Fascin expression in IPMN and its relationship with the clinicopathological features remain unclear, though IPMN has much in common with PanIN.

The aims of the present study were to analyze fascin expression using a large number of surgical IPMN specimens, to clarify its relationship with clinicopathological features including histological grade and phenotypic subtype, and to elucidate the association of fascin expression with progression of IPMNs.

Materials and methods

Patients and Tissue Specimens

A total of 116 samples of IPMN were used for the present study. All of the neoplasms were surgically resected at Kyushu University Hospital and its affiliated hospitals from 1986 to 2005. All specimens were cut into 5 mm stepwise tissue sections, and the gross features were recorded. For histopathological diagnosis, they were embedded in paraffin, and each of the serially cut sections, 4 μm in thickness, was stained with hematoxylin and eosin (H&E). On the basis of the greatest degree of dysplasia present, the lesions were classified as adenoma, borderline neoplasm, or carcinoma with or without invasion according to the World Health Organization (WHO) classification.[2] If present, invasive components were classified as tubular or mucinous noncystic (colloid) type. In accordance with the recently suggested subclassification system,[14] the lesions were also subclassified into four groups, gastric type, intestinal type, pancreatobiliary type, and oncocytic type, based on their histological phenotype and immunohistochemical expression of MUCs; gastric type MUC5AC+/MUC2−/MUC1−, intestinal type MUC5AC+/MUC2+/MUC1−, pancreatobiliary type MUC5AC+/MUC2−/MUC1+, and oncocytic type MUC5AC+/MUC2−/MUC1+. The subclassification was based primarily on histological phenotype and the immunolabeling for MUCs served as a confirmatory marker. IPMNs that could not be categorized specifically into one of the above four subtypes were segregated as unclassified type.

We also examined 10 cases of conventional pancreatic ductal adenocarcinoma for fascin expression, immunohistochemically. In addition, eight fresh-frozen samples of IPMN were obtained for quantitative analysis of fascin mRNA.

Immunohistochemistry

The primary antibodies used were follows as: anti-fascin (monoclonal, 55K-2; DAKO, CA, USA; 1:50 dilution), anti-MUC1 (Ma695; Novocastra Laboratories, Newcastle upon Tyne, UK; 1:200 dilution), anti-MUC2 (Ccp58; Novocastra Laboratories; 1:200 dilution), and anti-MUC5AC (CLH2; Novocastra Laboratories; 1:200 dilution). Sections were cut at 4 μm thickness from paraffin-embedded material, then dewaxed with xylene and rehydrated through a graded series of ethanol. After inhibition of endogenous peroxidase and antigen retrieval (microwave irradiation in citrate buffer for all the antibodies), sections were exposed to each primary antibody at 4°C overnight, and stained with a streptavidin–biotin–peroxidase kit (Nichirei, Tokyo, Japan). The sections were then finally reacted in 3,3′-diaminobenzidine, counterstained with hematoxylin, and mounted.

Evaluation of Immunohistochemical Staining of Fascin

Because IPMNs often show variability of epithelial dysplasia within the same tumor, immunohistochemical staining for fascin was evaluated within the area showing the highest degree of dysplasia in each neoplasm. The proportion of fascin positivity was measured using the following scale according to the percentage of fascin-positive tumor cells: <10%, 0; 10–30%, 1+; 30–60%, 2+; and >60%, 3+. Score 0 tumors were considered fascin-negative, whereas the others (1+ to 3+) were considered positive. All slides were evaluated independently by two investigators (HY and TI) without any prior knowledge of the patients' clinical information.

Microdissection and Extraction of Total RNA

We obtained total RNA from individual frozen samples using a laser microdissection system as

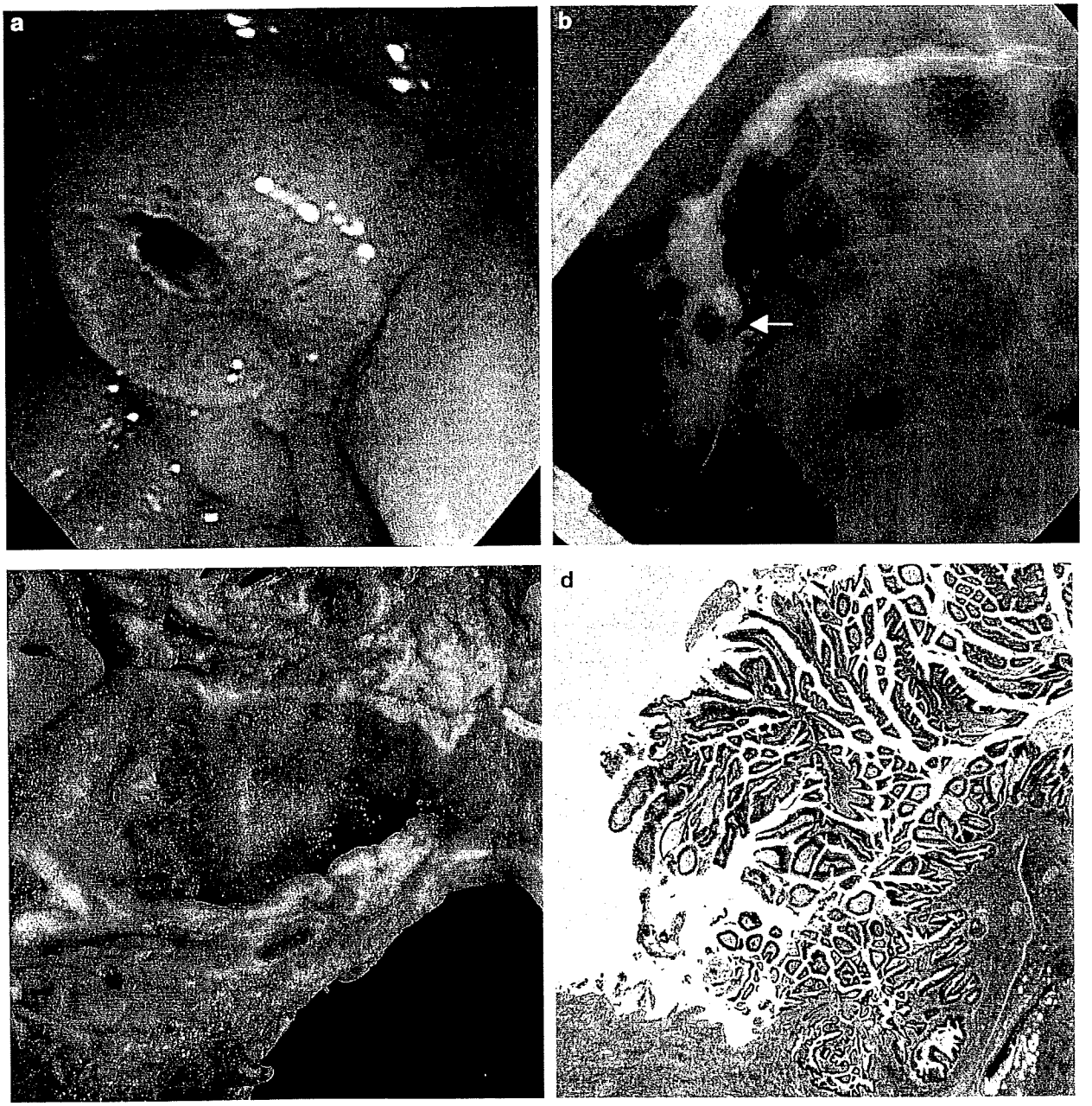

Figure 1 A representative case (75 years old, male) with typical findings of IPMN. **(a)** Endoscopic findings. Characteristic mucin extrusion through the ampulla of Vater. **(b)** Radiographic findings. Dilated main pancreatic duct (MPD) with mural nodule detected as a filling defect (arrow). **(c)** Macroscopic findings (MPD was opened at ventral side). Velvet-like appearance of the surface of a mural nodule. **(d)** Microscopic findings. Intraductal proliferation of neoplastic mucinous epithelium forming a papillary projection. Histological diagnosis is carcinoma.

described previously.[36] In brief, frozen tissue samples embedded in optimum cutting temperature compound (Sakura, Tokyo, Japan) were cut into 8-μm-thick sections. One section was stained with H&E for histological examination. IPMN cells were isolated selectively using laser microdissection and a pressure catapulting system (LMPC; Palm Microlaser Technologies AG, Bernried, Germany) in accordance with the manufacturer's protocols. After microdissection, total RNA was extracted from the selected cells according to the standard acid guanidinium thiocyanate–phenol–chloroform protocol[37] with glycogen (Funakoshi, Tokyo, Japan), and was subjected to real-time reverse-transcriptase polymerase chain reaction (RT-PCR) for quantitative measurement of fascin mRNA.

Quantitative Analysis of Fascin mRNA Expression by Real-Time RT-PCR

We designed a real-time RT-PCR protocol for the quantitative analysis of fascin mRNA and a refe-

rence gene, 18S ribosomal RNA (18S rRNA). We designed specific primers (fascin forward primer, 5′-gcaccctcaggtcaacatct-3′; reverse primer, 5′-aactccagc gtgtagccagt-3′; 18S rRNA forward primer, 5′-gatatgct catgtggtgttg-3′; reverse primer, 5′-aatcttcttcagtcgctc ca-3′), and used Basic Local Alignment Search Tool analysis to ensure the gene specificity of these primers. Quantitative one-step RT-PCR was carried out with a Quantitect SYBR Green RT-PCR kit (QIAGEN, Tokyo, Japan), and a LightCycler Quick System 350S (Roche Diagnostics, Mannheim, Germany), according to the manufacturers' instructions. In brief, the total volume of the reaction mixture was 20 μl, containing 10 μl of 2 × SYBR Green Buffer, 0.2 μl of RT mix, 1 μl of each primer (10 μmol/l), and 1 μl of total RNA. The reaction mixture was first incubated at 50°C for 15 min to allow reverse transcription. PCR was then initiated at 95°C for 10 min to activate modified Taq polymerase, followed by a 45-cycle amplification (95°C for 15 s, 55°C for 20 s, and 72°C for 10 s) and one cycle (95°C for 0 s, 65°C for 15 s, and 0.1°C/s to 99°C) for melting analysis. Each sample was run in triplicate. The mRNA expression of each gene was calculated on a standard curve constructed using total RNA from the MRC5 fibroblast cell line. For relative quantification, expression of fascin mRNA was normalized to that of 18S rRNA.

Table 1 Clinicopathologic findings of resected intraductal papillary mucinous neoplasms (IPMNs)

Parameters	*Number*
Age (years, mean ± s.d.)	66.34 ± 8.15
Sex	
Male	76 (66%)
Female	40 (34%)
Site	
Head	76 (66%)
Body and/or tail	39 (34%)
Tumor size (mm) (median (25, 75%))	30 (20, 40)
Mural nodule	
Absent	71 (61%)
Present	44 (38%)
Histological grade (WHO classification)	
Adenoma	45 (39%)
Borderline neoplasm	29 (25%)
Carcinoma	42 (36%)
Noninvasive	20 (17%)
Invasive	22 (19%)

s.d., standard deviation; WHO, World Health Organization.

Statistical Analysis

The χ^2 test was used to evaluate the association between histological grade and fascin expression. Fisher's exact test was used to assess the association between subtype and fascin expression or histological grade. After these analyses, multiple comparisons were carried out using Bonferroni's method. Spearman rank correlation analysis was used to study the relationship between histological grade and fascin score (0–3+). In the other analyses, the χ^2 test or Fisher's exact test was used for proportion, and the *t*-test, Mann–Whitney's *U*-test, analysis of variance, or the Kruskal–Wallis test was used for continuous data. *P*-values of less than 0.05 were considered statistically significant.

Results

Clinicopathological Features and Phenotypic Subclassification

A representative case showing typical endoscopic, radiographic, macroscopic and microscopic findings is shown in Figure 1. The clinicopathological findings from 116 cases are summarized in Table 1. Among the parameters, increasing tumor size ($P<0.0001$) and a presence of a mural nodule ($P<0.0001$) were significantly correlated with increased histological grade (adenoma–borderline neoplasm–carcinoma) (data not shown).

Of the 116 lesions, 59 (51%) were subclassified as gastric type, 39 (34%) as intestinal type, seven (6%)

Table 2 Subtype and histological grade (WHO classification)

	Adenoma	*Borderline*	*Carcinoma*			P
	n *(%)*	n *(%)*	n *(%)*	*Noninvasive*	*Invasive (tub:muc)*	
Sub-type						<0.0001
G-type ($n=59$)	41 (69)	13 (22)	5 (8)	1	4 (4:0)	
I-type* ($n=39$)	4 (10)	16 (41)	19 (49)	12	7 (3:4)	
PB-type* ($n=7$)	0 (0)	0 (0)	7 (100)	1	6 (6:0)	
O-type ($n=2$)	0 (0)	0 (0)	2 (100)	1	1 (1:0)	
U-type* ($n=9$)	0 (0)	0 (0)	9 (100)	5	4 (3:1)	

G-type, gastric type; I-type, intestinal type; muc, mucinous noncystic (colloid) invasive pattern; O-type, oncocytic type; PB-type, pancreatobiliary type; Tub, tubular invasive pattern; U-type, unclassified type.
*$P<0.05$ significantly increased histological grade compared with G-type, using Bonferroni's method.

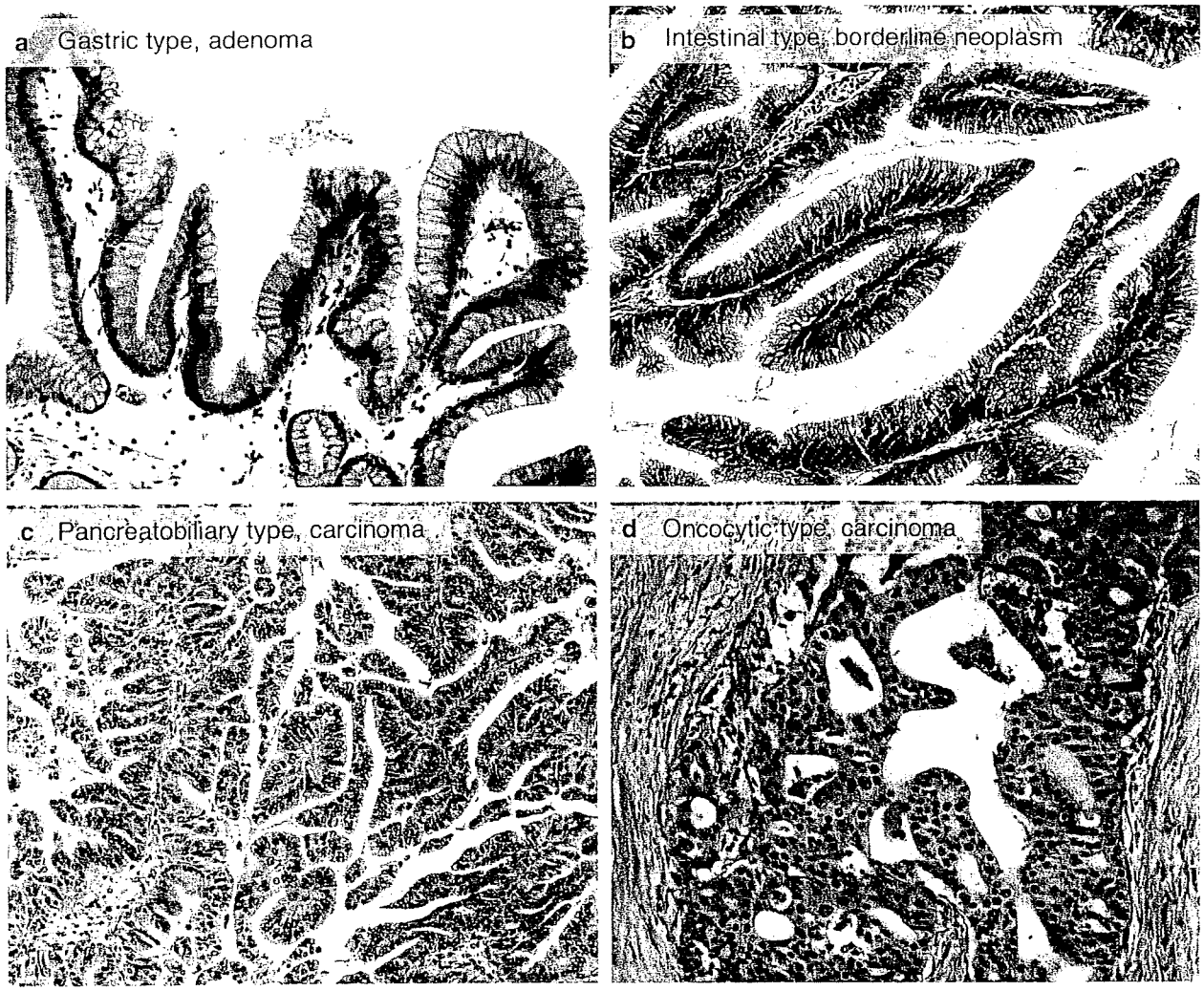

Figure 2 Representative images of the subtypes of IPMN stained with H&E. (**a**) Gastric-type IPMN consisting of cells resembling gastric foveolae with mild epithelial dysplasia. (**b**) Intestinal-type IPMN resembling intestinal villous neoplasms showing tall, columnar epithelial cells with moderate epithelial dysplasia. (**c**) Pancreatobiliary-type IPMN consisting of cells resembling cholangiopapillary neoplasms showing complex, thin, branching papillae with severe epithelial dysplasia. (**d**) Oncocytic-type IPMN consisting of cells with abundant, intensely eosinophilic cytoplasm and showing complex papillae with intraepithelial lumina and severe epithelial dysplasia.

as pancreatobiliary type, two (2%) as oncocytic type, and nine (8%) as unclassified type (Table 2). Each had characteristic papillae formation (Figure 2) and specific immunohistochemical reactivities for MUCs, as described previously.[14] All of the invasive components in the gastric-, pancreatobiliary-, and oncocytic-type neoplasms (four, six, and one neoplasms, respectively) displayed a tubular invasive pattern, whereas four of seven (57%) intestinal-type neoplasms and one of four (25%) unclassified-type neoplasms with invasive components showed a mucinous noncystic (colloid) invasive pattern. By multiple comparisons, intestinal-, pancreatobiliary-, and unclassified-type neoplasms showed significantly increased histological grade compared with gastric-type neoplasm ($P<0.05$; Table 2). Gastric-type neoplasms were significantly smaller (median diameter, 30 mm) than those of intestinal type (30 mm; $P<0.05$, data not shown).

Immunohistochemical Expression of Fascin

Of 116 IPMNs, 85 (73%) demonstrated positive immunohistochemical expression of fascin (Table 3). The immunohistochemical expression appeared as fine granular to diffuse cytoplasmic staining. In every slide prepared for immunohistochemistry, endothelial cells, lymphocytes, and stromal fibroblasts showed positive expression, and these were considered to be internal positive controls. Normal pancreatic ductal epithelium, acini, and islets of Langerhans were essentially nonreactive (Figure 3a); however, some parts of the hyperplastic ductal epithelium surrounding the IPMNs occasionally showed weak positivity for fascin. In addition, squamous metaplasia of the ductal epithelium was also weakly stained in one case. Compared with adenomas (23/45, 51%), the number of fascin-positive neoplasms was significantly higher among borderline neoplasms (25/29, 86%;

Table 3 Correlation between fascin expression and histological grade (WHO classification) or phenotypic subtype

Factor	*Fascin expression*		P
	−n (%)	*+ n (%)*	
Histological grade			<0.0001
Adenoma	22 (49)	23 (51)	
Borderline*	4 (14)	25 (86)	
Carcinoma*	5 (12)	37 (88)	
Phenotypic subtype			0.0005
G-type	23 (39)	36 (61)	
I-type**	4 (10)	35 (90)	
PB-type	2 (29)	5 (71)	
O-type	2 (100)	0 (0)	
U-type	0 (0)	9 (100)	
Total	31 (27)	85 (73)	

G-type, gastric type; I-type, intestinal type; O-type, oncocytic type; PB-type, pancreatobiliary type; U-type, unclassified type.
*$P<0.05$ compared with adenoma, using Bonferroni's method.
**$P<0.05$ compared with gastric type, using Bonferroni's method.

$P<0.05$) and carcinomas (37/42, 88%; $P<0.05$) (Table 3, Figure 3b–d). No difference was observed between borderline neoplasms and carcinomas. The fascin score was significantly raised in relation to increased histological grade (Figure 4; $P<0.001$). Within each neoplasm, high-grade-areas often showed more diffuse and intense immunoreactivity for fascin than low grade-areas (Figure 3e). All invasive components seen in the slides prepared for immunohistochemical staining were positive for fascin in both tubular and mucinous noncystic (colloid) patterns (Figure 3f). Intestinal-type neoplasms were more frequently positive for fascin (35/39, 90%) than gastric-type neoplasms (36/59, 61%) ($P<0.05$; Table 3). Two oncocytic-type neoplasms were both negative for fascin. Several parameters (age, sex, tumor site, tumor size, and absence or presence of mural nodule) had no correlation with fascin expression (data not shown).

Of the conventional pancreatic ductal adenocarcinomas, 90% (9 of 10) showed diffuse and intense fascin positivity (Figure 3h), the rate being as high as previously reported.[30,31]

Expression of Fascin mRNA

To confirm the fascin overexpression demonstrated by immunohistochemistry and to assess whether the overexpression was transcriptional or post-transcriptional, real-time RT-PCR for quantitative evaluation of fascin mRNA was performed, using frozen samples of IPMNs. A laser microdissection system was used to isolate IPMN cells for the following purposes: (1) to collect selectively the neoplastic cells showing the same degree of dysplasia within a neoplasm; and (2) to avoid contamination with stromal tissue, which contains many endothelial cells and/or fibroblasts that normally express fascin. The eight frozen samples comprised four samples of mild epithelial dysplasia (corresponding to adenoma) and four of moderate to severe epithelial dysplasia (borderline neoplasm to carcinoma).

The relative expression of fascin mRNA of each sample evaluated by real-time PCR is shown in Figure 5. A tendency was recognized whereby fascin mRNA levels in moderately to severely dysplastic epithelium were higher than those in mildly dysplastic epithelium, though the difference was not statistically significant, possibly because of the small number of samples. These data were consistent with the results of immunohistochemistry, and suggested that the overexpression of fascin in IPMNs was transcriptional.

Discussion

In the present study, we found that fascin was upregulated in the majority (73%) of IPMNs and was correlated with increased histological grade. These findings suggest that fascin overexpression is involved in the progression of IPMN. To our knowledge, this is the first report to reveal fascin overexpression and its association with clinicopathological features in IPMNs, and to evaluate quantitatively the expression of fascin mRNA in human neoplasms using laser microdissection and real time RT-PCR.

Fascin is a well-conserved actin-regulatory protein. *In vitro* experiments have indicated that it is involved in cellular processes such as motility,[27,38,39] loss of cell–cell contact in relation to adhesion molecules,[39–41] and cell proliferation.[25,27] From these observations, it may be presumed that fascin may play an important role in cellular malignant transformation. Indeed, in a variety of human carcinomas, fascin expression is consistently associated with the clinical aggressiveness of the tumor.[18,19,21,23,24,26,33]

Among the pancreatic neoplasms, Iacobuzio-Donahue *et al*[42] reported fascin upregulation for the first time in ductal adenocarcinoma using cDNA microarrays (13-fold overexpression of fascin transcripts in ductal adenocarcinoma compared with normal tissues). Immunohistochemical studies then confirmed fascin overexpression, not only in infiltrating ductal adenocarcinomas[28,30,31] but also in PanINs.[29,30] The fact that PanINs show fascin upregulation correlated with histological grade increased our interest in fascin expression in IPMNs, because PanINs and IPMNs share the following fundamental characteristics:[5,6] inherently intraductal; composed predominantly of columnar, mucin-producing cells that may grow in a flat configuration or may produce papillae; exhibit a range of cytologic and architectural atypia (mild, moderate and severe); recognized as precursors to

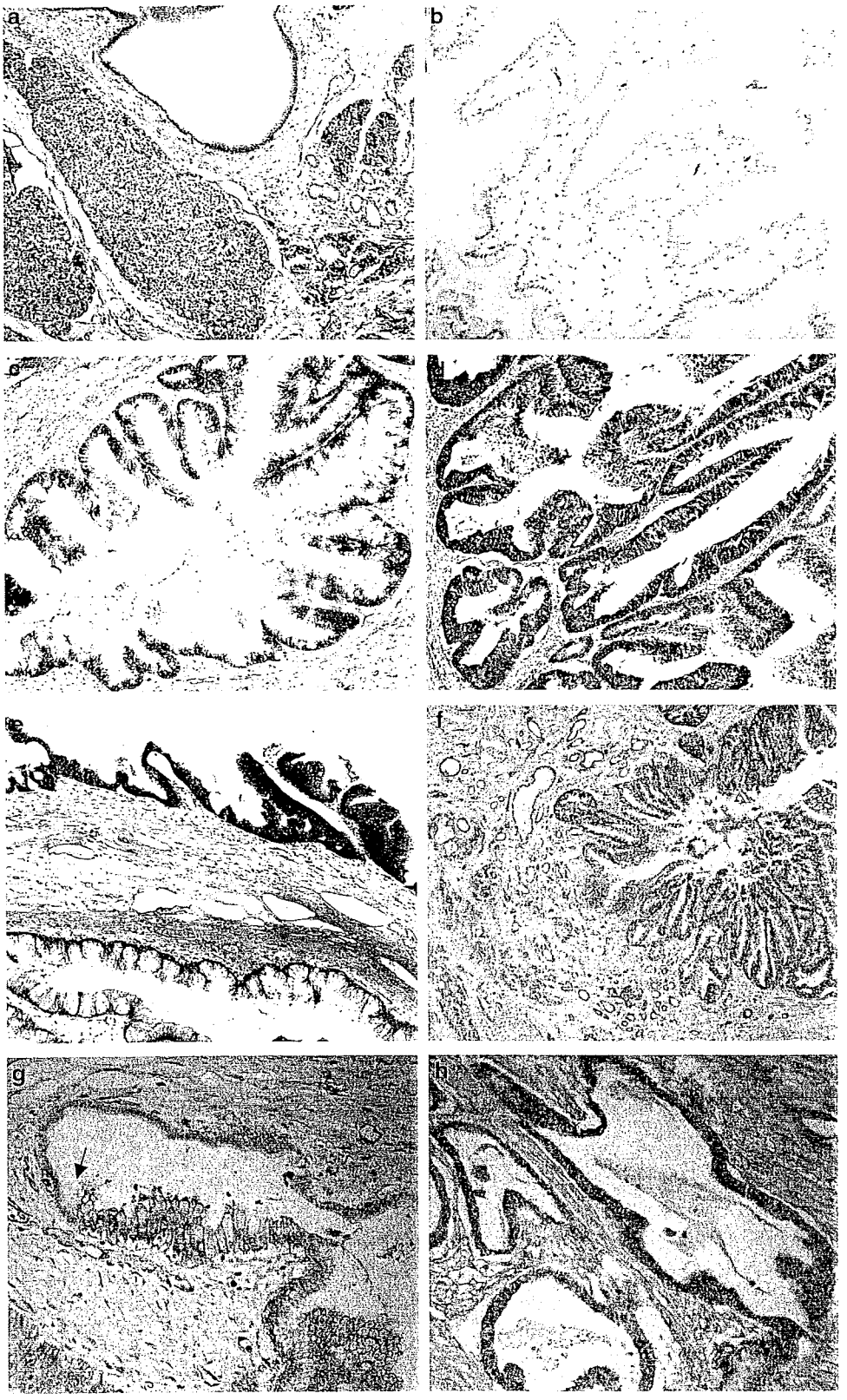

Figure 3 Fascin expression on immunohistochemistry. (**a**) Negative for normal pancreatic ductal epithelium, acini, and islets of Langerhans, whereas positive for endothelial cells and stromal fibroblasts (internal control). (**b**) Negative case of adenoma (score 0). (**c**) Positive case of borderline neoplasm (score 3+). (**d**) Positive case of carcinoma (score 3+). (**e**) Diffuse and intense reactivity in moderately to severely dysplastic epithelium (upper), with weak and basally localized reactivity in mildly dysplastic epithelium (lower) within a neoplasm. (**f**) Positive for both intraepithelial components (right upper) and invasive components (left lower). (**g**) Abrupt transition (arrow) from fascin-positive neoplastic epithelium to fascin-negative normal duct epithelium. (**h**) Diffuse and intense positivity in conventional pancreatic ductal adenocarcinoma.

invasive adenocarcinoma; and sequentially accumulate similar genetic alterations with increasing cytoarchitectural atypia.[43–45]

We showed that fascin overexpression in IPMNs was correlated with increased histological grade by immunohistochemical analysis, followed by a supporting molecular experiment that showed upregulation of fascin mRNA. We consider that fascin upregulation would be a relatively early event in the progression of IPMN, because of the finding that fascin expression was significantly and almost equally greater in borderline neoplasms (86%) and carcinomas (88%) than in adenomas (51%). It would be interesting to compare these results with findings for PanINs. In an immunohistochemical study, Maitra *et al*[30] detected focal or diffuse cytoplasmic fascin expression in 25% of PanIN-1A, 28% of PanIN-1B, 57% of PanIN-2, and 57% of PanIN-3,

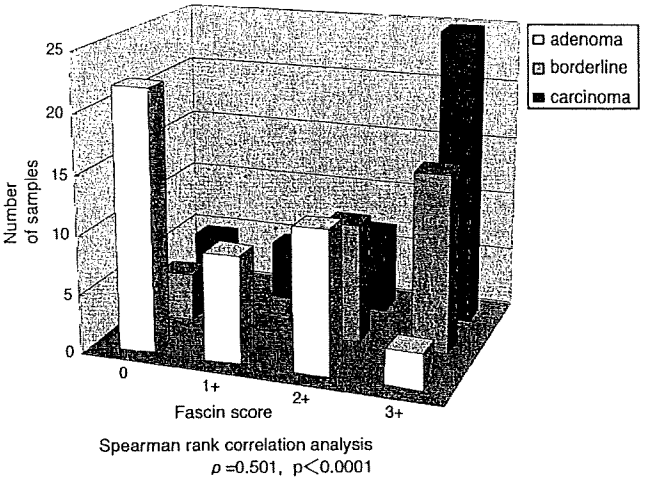

Figure 4 Correlation between histological grade and fascin score. Fascin score was significantly raised in relation to increased histological grade.

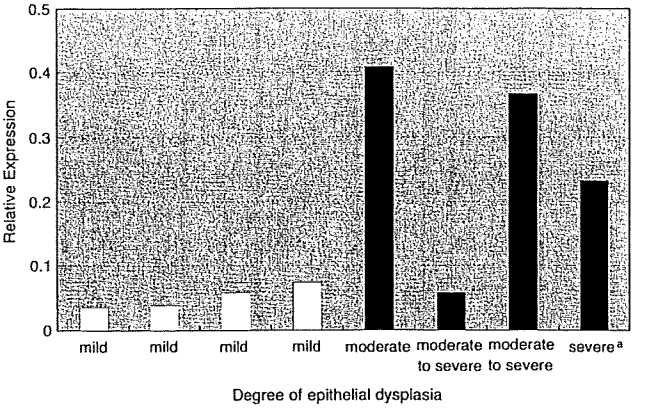

Figure 5 Relative expression of fascin mRNA evaluated by real-time RT-PCR. The relative expression of fascin in eight frozen samples was normalized to18s rRNA. Higher in moderately to severely dysplastic epithelium (black) than in mildly dysplastic epithelium (white). [a]Severe dysplasia with a little invasive components.

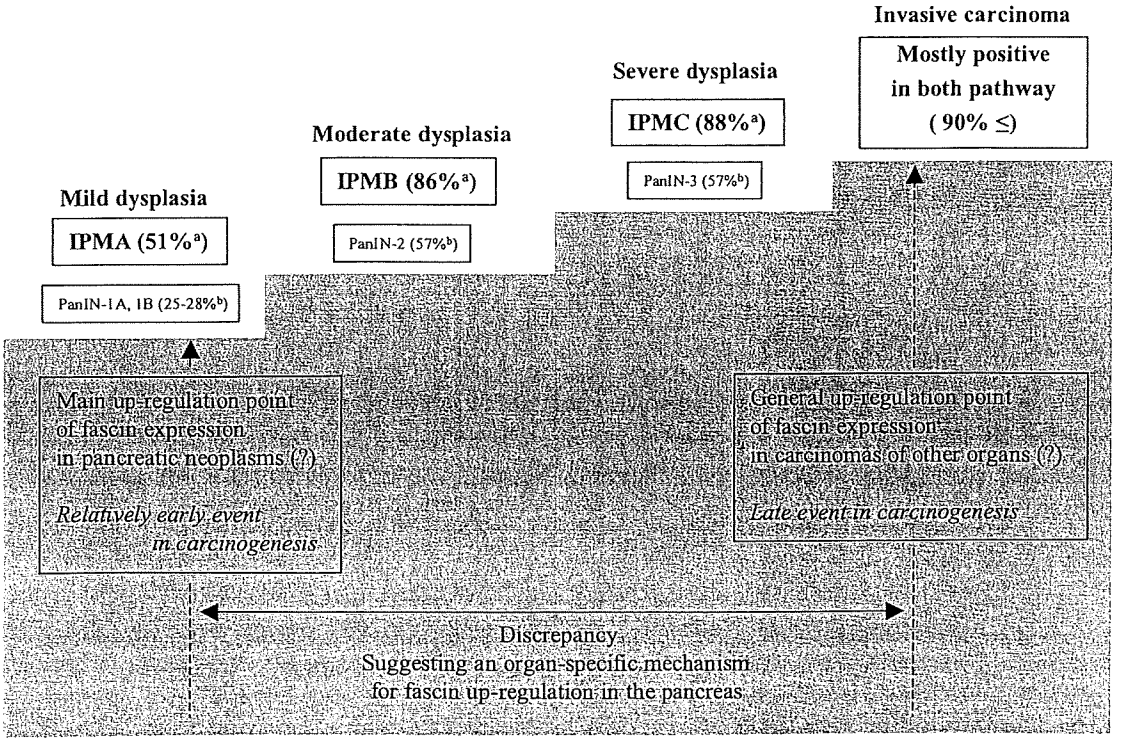

Figure 6 Hypothesis for fascin upregulation in multi-step carcinogenesis of pancreatic neoplasms. IPMA, intraductal papillary mucinous adenoma; IPMB, borderline IPMN; IPMC, intraductal papillary mucinous carcinoma. [a]Percentage of fascin-positive IPMNs documented in the present study. [b]Percentage of fascin-positive pancreatic intraepithelial neoplasms documented in Maitra *et al*.[30]

and described fascin upregulation as an 'intermediate' event in pancreatic adenocarcinoma progression. Their results and ours suggest that upregulation of fascin occurs in similar stage (relatively early phase) in tumorigenesis of both IPMNs and PanINs (Figure 6). It remains to be seen whether fascin expression represents merely a surrogate marker of histological grade, or whether it plays a pathogenic role in tumorigenesis and the progression of IPMNs. Using RNA interference, it has been shown recently that down-regulation of fascin has inhibitory effects on the migration, proliferation and invasiveness of esophageal squamous cell carcinoma cell lines.[24,25] These data suggest that fascin itself contributes to tumor progression, and raise the possibility that fascin could be a novel therapeutic target.

A previous report suggested that a pathway for fascin upregulation was dependent on amplification or overexpression of c-erbB-2/HER-2.[20] Others have shown a possible influence of Wnt signaling on fascin activity, suggesting that anomalies of this pathway may upregulate fascin expression in cancer cells.[40] However, the mechanism of fascin upregulation in IPMN is not known, because neither c-erbB-2 amplification nor Wnt signaling abnormalities are particularly common in IPMN. We consider that there is an organ-specific mechanism for fascin upregulation in the pancreas, because invasive pancreatic adenocarcinomas express prominently high levels of fascin compared with other carcinomas. In addition, IPMNs and PanINs frequently show fascin expression though they are both intraepithelial lesions. Fascin upregulation is not frequently recognized in intraepithelial neoplasms of other organs (Figure 6).

We also performed phenotypic subclassification of IPMNs, and re-confirmed the findings described previously. Gastric types usually showed mild dysplasia and intestinal types showed moderate to severe dysplasia, whereas pancreatobiliary and oncocytic types showed severe dysplasia corresponding to carcinoma *in situ*;[8,10,14] intestinal-type neoplasms were more frequently associated with a mucinous noncystic (colloid) invasive pattern compared with other types;[4,7–9,12] and the oncocytic type was a rare variant.[46] With regard to the relationship between fascin expression and the phenotypic subclassification, fascin overexpression occurred more frequently in intestinal-type neoplasms (90%) than in the gastric type (61%) by multiple comparisons. In contrast, intestinal-type neoplasms exhibited a higher histological grade than the gastric type. It remains unclear whether the difference in fascin overexpression in gastric- and intestinal-type neoplasms is affected by their histological grade, or whether there is a more essential mechanical association between fascin overexpression and subtype. For example, MUC variation may have some molecular relation to fascin expression that has not been documented. Interestingly, two oncocytic-type neoplasms in the present study were both fascin-negative, though they showed severely dysplastic epithelium corresponding to carcinoma. This may indicate that the progression pathway of oncocytic-type neoplasms differs from that of the other types in parts.

In conclusion, overexpression of fascin is correlated with increased histological grade of IPMN and occurs relatively early in the pathogenesis of IPMN. Fascin may provide a new cancer prevention strategy as a possible therapeutic molecular target to inhibit the progression of IPMNs.

References

1 Ohhashi K, Murakami Y, Takekoshi T, *et al.* Four cases of 'mucin producing' cancer of the pancreas on specific findings of the papilla of Vater (Abstract). Prog Diagn Endosc 1982;20:348–351.
2 Longnecker DS, Adler G, Hruban RH, *et al.* Intraductal papillary-mucinous neoplasms of the pancreas. In: Hamilton SR, Aaltonen LA (eds). World Health Organization Classification of Tumours. Pathology and Genetics of Tumours of the Digestive System. IARC Press: Lyon, France, 2000, pp 237–240.
3 Solcia E, Capella C, Klöppel G. Atlas of Tumor Pathology: Tumors of the Pancreas, 3rd Series Fascicle. Armed Forces Institute of Pathology: Washington, DC, 1997.
4 Adsay NV, Merati K, Andea A, *et al.* The dichotomy in the preinvasive neoplasia to invasive carcinoma sequence in the pancreas: differential expression of MUC1 and MUC2 supports the existence of two separate pathways of carcinogenesis. Mod Pathol 2002; 15:1087–1095.
5 Hruban RH, Adsay NV, Albores-Saavedra J, *et al.* Pancreatic intraepithelial neoplasia: a new nomenclature and classification system for pancreatic duct lesions. Am J Surg Pathol 2001;25:579–586.
6 Hruban RH, Takaori K, Klimstra DS, *et al.* An illustrated consensus on the classification of pancreatic intraepithelial neoplasia and intraductal papillary mucinous neoplasms. Am J Surg Pathol 2004;28: 977–987.
7 Adsay NV, Conlon KC, Zee SY, *et al.* Intraductal papillary-mucinous neoplasms of the pancreas: an analysis of *in situ* and invasive carcinomas in 28 patients. Cancer 2002;94:62–77.
8 Adsay NV, Merati K, Basturk O, *et al.* Pathologically and biologically distinct types of epithelium in intraductal papillary mucinous neoplasms: delineation of an 'intestinal' pathway of carcinogenesis in the pancreas. Am J Surg Pathol 2004;28:839–848.
9 Fukushima N, Mukai K, Kanai Y, *et al.* Intraductal papillary tumors and mucinous cystic tumors of the pancreas: clinicopathologic study of 38 cases. Hum Pathol 1997;28:1010–1017.
10 Nakamura A, Horinouchi M, Goto M, *et al.* New classification of pancreatic intraductal papillary-mucinous tumour by mucin expression: its relationship with potential for malignancy. J Pathol 2002;197: 201–210.
11 Yonezawa S, Horinouchi M, Osako M, *et al.* Gene expression of gastric type mucin (MUC5AC) in pancreatic tumors: its relationship with the biological behavior of the tumor. Pathol Int 1999;49:45–54.

12 Yonezawa S, Nakamura A, Horinouchi M, *et al.* The expression of several types of mucin is related to the biological behavior of pancreatic neoplasms. J Hepatobiliary Pancreat Surg 2002;9:328–341.
13 Yonezawa S, Taira M, Osako M, *et al.* MUC-1 mucin expression in invasive areas of intraductal papillary mucinous tumors of the pancreas. Pathol Int 1998;48: 319–322.
14 Furukawa T, Kloppel G, Volkan Adsay N, *et al.* Classification of types of intraductal papillary-mucinous neoplasm of the pancreas: a consensus study. Virchows Arch 2005;447:794–799.
15 Adams JC. Roles of fascin in cell adhesion and motility. Curr Opin Cell Biol 2004;16:590–596.
16 Hashimoto Y, Skacel M, Adams JC. Roles of fascin in human carcinoma motility and signaling: prospects for a novel biomarker? Int J Biochem Cell Biol 2005;37: 1787–1804.
17 Kureishy N, Sapountzi V, Prag S, *et al.* Fascins, and their roles in cell structure and function. Bioessays 2002;24:350–361.
18 Pelosi G, Pasini F, Fraggetta F, *et al.* Independent value of fascin immunoreactivity for predicting lymph node metastases in typical and atypical pulmonary carcinoids. Lung Cancer 2003;42:203–213.
19 Pelosi G, Pastorino U, Pasini F, *et al.* Independent prognostic value of fascin immunoreactivity in stage I nonsmall cell lung cancer. Br J Cancer 2003;88:537–547.
20 Grothey A, Hashizume R, Ji H, *et al.* C-erbB-2/ HER-2 upregulates fascin, an actin-bundling protein associated with cell motility, in human breast cancer cell lines. Oncogene 2000;19:4864–4875.
21 Grothey A, Hashizume R, Sahin AA, *et al.* Fascin, an actin-bundling protein associated with cell motility, is upregulated in hormone receptor negative breast cancer. Br J Cancer 2000;83:870–873.
22 Rodriguez-Pinilla SM, Sarrio D, Honrado E, *et al.* Prognostic significance of basal-like phenotype and fascin expression in node-negative invasive breast carcinomas. Clin Cancer Res 2006;12:1533–1539.
23 Yoder BJ, Tso E, Skacel M, *et al.* The expression of fascin, an actin-bundling motility protein, correlates with hormone receptor-negative breast cancer and a more aggressive clinical course. Clin Cancer Res 2005; 11:186–192.
24 Hashimoto Y, Ito T, Inoue H, *et al.* Prognostic significance of fascin overexpression in human esophageal squamous cell carcinoma. Clin Cancer Res 2005;11: 2597–2605.
25 Xie JJ, Xu LY, Zhang HH, *et al.* Role of fascin in the proliferation and invasiveness of esophageal carcinoma cells. Biochem Biophys Res Commun 2005;337: 355–362.
26 Hashimoto Y, Shimada Y, Kawamura J, *et al.* The prognostic relevance of fascin expression in human gastric carcinoma. Oncology 2004;67:262–270.
27 Jawhari AU, Buda A, Jenkins M, *et al.* Fascin, an actin-bundling protein, modulates colonic epithelial cell invasiveness and differentiation *in vitro*. Am J Pathol 2003;162:69–80.
28 Lu Z, Hu L, Evers S, *et al.* Differential expression profiling of human pancreatic adenocarcinoma and healthy pancreatic tissue. Proteomics 2004;4:3975–3988.
29 Maitra A, Adsay NV, Argani P, *et al.* Multicomponent analysis of the pancreatic adenocarcinoma progression model using a pancreatic intraepithelial neoplasia tissue microarray. Mod Pathol 2003;16:902–912.
30 Maitra A, Iacobuzio-Donahue C, Rahman A, *et al.* Immunohistochemical validation of a novel epithelial and a novel stromal marker of pancreatic ductal adenocarcinoma identified by global expression microarrays: sea urchin fascin homolog and heat shock protein 47. Am J Clin Pathol 2002;118:52–59.
31 Swierczynski SL, Maitra A, Abraham SC, *et al.* Analysis of novel tumor markers in pancreatic and biliary carcinomas using tissue microarrays. Hum Pathol 2004;35:357–366.
32 Van Heek NT, Maitra A, Koopmann J, *et al.* Gene expression profiling identifies markers of ampullary adenocarcinoma. Cancer Biol Ther 2004;3:651–656.
33 Hu W, McCrea PD, Deavers M, *et al.* Increased expression of fascin, motility associated protein, in cell cultures derived from ovarian cancer and in borderline and carcinomatous ovarian tumors. Clin Exp Metastasis 2000;18:83–88.
34 Tong GX, Yee H, Chiriboga L, *et al.* Fascin-1 expression in papillary and invasive urothelial carcinomas of the urinary bladder. Hum Pathol 2005;36:741–746.
35 Goncharuk VN, Ross JS, Carlson JA. Actin-binding protein fascin expression in skin neoplasia. J Cutan Pathol 2002;29:430–438.
36 Tachikawa T, Irie T. A new molecular biology approach in morphology: basic method and application of laser microdissection. Med Electron Microsc 2004;37:82–88.
37 Chomczynski P, Sacchi N. Single-step method of RNA isolation by acid guanidinium thiocyanate-phenol-chloroform extraction. Anal Biochem 1987;162:156–159.
38 Adams JC, Schwartz MA. Stimulation of fascin spikes by thrombospondin-1 is mediated by the GTPases Rac and Cdc42. J Cell Biol 2000;150:807–822.
39 Yamashiro S, Yamakita Y, Ono S, *et al.* Fascin, an actin-bundling protein, induces membrane protrusions and increases cell motility of epithelial cells. Mol Biol Cell 1998;9:993–1006.
40 Tao YS, Edwards RA, Tubb B, *et al.* beta-Catenin associates with the actin-bundling protein fascin in a noncadherin complex. J Cell Biol 1996;134:1271–1281.
41 Wong V, Ching D, McCrea PD, *et al.* Glucocorticoid down-regulation of fascin protein expression is required for the steroid-induced formation of tight junctions and cell–cell interactions in rat mammary epithelial tumor cells. J Biol Chem 1999;274: 5443–5453.
42 Iacobuzio-Donahue CA, Maitra A, Shen-Ong GL, *et al.* Discovery of novel tumor markers of pancreatic cancer using global gene expression technology. Am J Pathol 2002;160:1239–1249.
43 Biankin AV, Biankin SA, Kench JG, *et al.* Aberrant p16(INK4A) and DPC4/Smad4 expression in intraductal papillary mucinous tumours of the pancreas is associated with invasive ductal adenocarcinoma. Gut 2002;50:861–868.
44 Sato N, Ueki T, Fukushima N, *et al.* Aberrant methylation of CpG islands in intraductal papillary mucinous neoplasms of the pancreas. Gastroenterology 2002;123:365–372.
45 Soldini D, Gugger M, Burckhardt E, *et al.* Progressive genomic alterations in intraductal papillary mucinous tumours of the pancreas and morphologically similar lesions of the pancreatic ducts. J Pathol 2003;199: 453–461.
46 Adsay NV, Adair CF, Heffess CS, *et al.* Intraductal oncocytic papillary neoplasms of the pancreas. Am J Surg Pathol 1996;20:980–994.

S100A6 Is Increased in a Stepwise Manner during Pancreatic Carcinogenesis: Clinical Value of Expression Analysis in 98 Pancreatic Juice Samples

Kenoki Ohuchida,[1] Kazuhiro Mizumoto,[1] Jun Yu,[1] Hiroshi Yamaguchi,[2] Hiroyuki Konomi,[1] Eishi Nagai,[1] Koji Yamaguchi,[1] Masazumi Tsuneyoshi,[2] and Masao Tanaka[1]

[1]Department of Surgery and Oncology and [2]Department of Anatomic Pathology, Graduate School of Medical Sciences, Kyushu University, Fukuoka, Japan

Abstract

There are few reports describing the diagnostic significance of *S100A6* expression in clinical samples obtained from patients with pancreatic disease. In the present study, we measured *S100A6* expression in pancreatic tissues and juice to evaluate its involvement in pancreatic carcinogenesis. We did quantitative real-time reverse transcription-PCR to measure mRNA expression in microdissected cells and pancreatic juice samples. Microdissected invasive ductal carcinoma and intraductal papillary mucinous neoplasm (IPMN) cells expressed significantly higher levels of *S100A6* than did microdissected pancreatitis-affected epithelial and normal cells (all comparison; $P < 0.008$). Median levels of *S100A6* in invasive ductal carcinoma were higher than those in IPMN, and those in pancreatitis-affected epithelial cells tended to be higher than those in normal cells, although these differences were not statistically significant. In analyses of pancreatic juice, IPMN and pancreatic cancer samples expressed significantly higher levels of *S100A6* than did chronic pancreatitis samples (both; $P < 0.017$), but levels in pancreatic cancer and IPMN samples did not differ form each other. Receiver operating characteristic (ROC) curve analysis revealed that measurement of *S100A6* was useful for discriminating cancer (area under the ROC curve, 0.864) or IPMN (area under the ROC curve, 0.749) from chronic pancreatitis. The present data suggest that expression of *S100A6* is increased in a stepwise manner during pancreatic carcinogenesis and may be a biomarker for evaluating malignant potential. Measurement of *S100A6* in pancreatic juice may be useful to detect early pancreatic cancer or identify individuals with high-risk lesions that may progress to pancreatic cancer. (Cancer Epidemiol Biomarkers Prev 2007;16(4):649–54)

Introduction

Pancreatic cancer is considered one of the most lethal forms of cancer because it is difficult to diagnose early and it is resistant to conventional therapies (1). The major symptoms at presentation are not sufficiently diagnostic because they are consistent with benign or inflammatory disease processes.

The importance of distinguishing pancreatic cancer and chronic pancreatitis is highlighted by reports that 5% to 10% of resected pancreatic tissues are eventually determined to be pancreatitis rather than pancreatic cancer (2). However, there is considerable overlap of the symptoms and clinical data for pancreatic cancer and pancreatitis. This overlap may in part reflect the potential for pancreatic cancer to arise in an environment of pancreatitis and the ability of pancreatic cancer to induce secondary inflammatory processes.

Cystic lesions of the pancreas are being detected with increasing frequency due to application of advanced diagnostic imaging technologies. Intraductal papillary mucinous neoplasm (IPMN) is the most common cystic neoplasm of the pancreas and was described initially by Ohhashi et al. (3) in 1982. IPMN is a precursor lesion of a subset of pancreatic cancer and is often associated with pancreatic cancer occurring as a separate lesion or as carcinoma derived from IPMN (4). Thus, it is important to distinguish pancreatic cancer from IPMN as well as from chronic pancreatitis.

Despite improvements in diagnostic modalities, it is still difficult to distinguish a small, resectable pancreatic cancer from chronic pancreatitis or IPMN. Early detection and diagnosis of pancreatic cancer would certainly improve patient survival. Therefore, novel screening and diagnostic tools are needed.

We and other investigators reported that both S100A6 mRNA and protein are overexpressed in pancreatic cancer (5-7), suggesting that S100A6 may be a promising diagnostic marker of pancreatic cancer. Although the role of S100A6 has yet to be clearly defined, it has been implicated in several cellular processes, such as cell proliferation and invasion (5, 8). In our previous study, we showed that *S100A6* is differentially expressed between normal epithelial ductal cells or pancreatic intraepithelial neoplasia (PanIN), which is a precursor lesion of pancreatic cancer (9), and invasive ductal carcinoma (IDC; ref. 5). In the present study, to refine our understanding of the involvement of *S100A6* in pancreatic carcinogenesis, we analyzed *S100A6* expression in IPMN and pancreatitis-affected epithelial (PAE) cells, only small percentage of which have the potential to progress to pancreatic cancer (10, 11). In addition, to clarify the clinical significance of *S100A6* mRNA expression in clinical samples, such as pancreatic juice, we used one-step quantitative real-time reverse transcription-PCR (RT-PCR) with gene-specific priming, short amplicons, and normalization to reference genes. It was reported recently that gene expression could be measured reliably from degraded RNA with this procedure (12-14). We successfully measured *S100A6* expression from degraded RNA in pancreatic juice samples from patients with IPMN and compared expression levels with those in pancreatic juice from patients with pancreatic cancer or chronic pancreatitis.

Received 2/27/06; revised 11/6/06; accepted 1/25/07.

Grant support: Grant-in-Aid from the Ministry of Education, Culture, Sports, Science and Technology of Japan, Japan Society for the Promotion of Science for Young Scientists Research Fellowships, and Japanese Foundation for Research and Promotion of Endoscopy grant.

The costs of publication of this article were defrayed in part by the payment of page charges. This article must therefore be hereby marked *advertisement* in accordance with 18 U.S.C. Section 1734 solely to indicate this fact.

Requests for reprints: Kazuhiro Mizumoto, Department of Surgery and Oncology, Graduate School of Medical Sciences, Kyushu University, 3-1-1 Maidashi, Fukuoka 812-8582, Japan. Phone: 81-92-642-5440; Fax: 81-92-642-5458. E-mail: mizumoto@med.kyushu-u.ac.jp

Copyright © 2007 American Association for Cancer Research.

doi:10.1158/1055-9965.EPI-06-0157

Materials and Methods

Pancreatic Tissues and Pancreatic Juice. Tissue samples were obtained from the primary tumor of each resected pancreas or from peripheral tissues away from the tumor at the time of surgery at Kyushu University Hospital (Fukuoka, Japan) as described previously (15). Experienced pathologists did histologic examination of all tissues adjacent to the specimens. Pancreatic juice samples were collected from 102 patients with various pancreatic diseases and 5 patients without pancreatic disease who underwent endoscopic retrograde cholangiopancreatography for suspected malignancy of the pancreas at Kyushu University Hospital between January 1, 2002 and August 31, 2005 as described previously (16). We used pellets of cellular material from pancreatic juice for preparation of RNAs. We eventually excluded the data of nine samples in the pancreatic juice analyses. Three of these nine samples were excluded because neither signals for *S100A6* nor *β-actin* was detected with real-time RT-PCR, possibly due to improper sampling, handling, or storage of samples. Two of the remaining six samples were excluded because of DNA contamination, which was confirmed by RT-minus experiments. The remaining four samples, which were from pancreatitis-affected pancreata, were excluded because *S100A6* could not be measured quantitatively, although *β-actin* expression was detected. Therefore, the final samples included 98 pancreatic juice specimens, including 26 from patients with pancreatic cancer, 37 from patients with nonmalignant IPMNs, 30 from patients with chronic pancreatitis, and 5 from patients who underwent endoscopic retrograde cholangiopancreatography to rule out pancreatic disease and were then diagnosed with diseases other than pancreatic disease. The diagnosis of pancreatic ductal adenocarcinoma was confirmed by histologic examination of resected specimens when available, but when the case was inoperable, a clinical diagnosis was made based on imaging findings and the subsequent outcome of the patient. Staging of pancreatic cancer was done according to the Japan Pancreas Society classification (17). Chronic pancreatitis or IPMN was diagnosed based on histologic examination of resected specimens or clinical findings at the time of the initial diagnosis and during a follow-up period of at least 12 months that included conventional diagnostic imaging. Cytologic examination was done by experienced cytologists according to the classification described previously (18). Class I comprised benign and nonneoplastic epithelium with no or only slight dysplasia. Class II comprised regenerative or neoplastic epithelium with slight dysplasia. Class III included neoplastic epithelium with mild dysplasia corresponding to adenoma. Class IV contained neoplastic epithelium with moderate dysplasia highly suggestive of adenocarcinoma. Class V was unequivocal malignant epithelium corresponding to adenocarcinoma. Written informed consent was obtained from all patients, and the study was approved by our institution's surveillance committee and conducted according to the Helsinki Declaration.

Isolation of Total RNA. Total RNA was extracted from cell pellets of pancreatic juice according to the standard acid guanidinium thiocyanate-phenol-chloroform protocol (19) with glycogen (Funakoshi, Tokyo, Japan) and from cells isolated by laser microdissection with a PicoPure RNA Isolation kit (Arcturus Bioscience, Mountain View, CA) with DNase I (Roche Diagnostics, Mannheim, Germany) treatment according to the manufacturers' instructions. RNA concentrations in extracts were measured in a NanoDrop ND-1000 spectrophotometer (NanoDrop Technologies, Inc., Rockland, DE), determining the absorbance at 260 and 280 nm ($A_{260/280}$). RNA integrity was assessed with an Agilent Bioanalyzer 2100 (Agilent, Palo Alto, CA).

Quantitative Analysis of S100A6 mRNA Levels by One-step Real-time RT-PCR with Gene-Specific Priming. We used one-step quantitative real-time RT-PCR with gene-specific priming to examine mRNA levels in various types of clinical samples, which contain weakly or extensively fragmented RNA. A major advantage of this technology is its ability to measure gene expression reliably from fragmented RNA through synthesis of cDNA with gene-specific primers and utilization of short amplicons and normalization (12–14). We used specific primers for *S100A6* and *β-actin* as described previously (5). One-step quantitative real-time RT-PCR with gene-specific priming was done with a QuantiTect SYBR Green RT-PCR kit (Qiagen, Tokyo, Japan) with a LightCycler Quick System 350S (Roche Diagnostics). The reaction mixture was first incubated at 50°C for 15 min to allow for reverse transcription, where first-strand cDNA was synthesized with a gene-specific primer. PCR was initiated with one cycle of 95°C for 10 min to activate the modified Taq polymerase followed by 45 cycles of 94°C for 15 s, 55°C for 20 s, and 72°C for 10 s and one cycle of 95°C for 0 s, 65°C for 15 s, and +0.1°C/s to 95°C for melting analysis to visualize nonspecific PCR products because different fragments appear as separate distinct melting peaks. Each primer set used in the present study produced a single melting peak and a single prominent band of the expected size on microchip electrophoresis. To confirm the presence of DNA contamination, we did RT-PCR with or without reverse transcriptase. Each sample was run twice, and any sample showing a greater than 10% deviation in the RT-PCR value was tested a third time. Levels of mRNA in each sample were calculated from a standard curve generated with total RNA from Capan-1 human pancreatic cancer cells. Expression of *S100A6* mRNA was normalized to that of *β-actin*.

Microdissection-Based Quantitative Analysis of S100A6 mRNA. Frozen tissue samples were cut into 8-μm-thick sections. One section was stained with H&E for histologic examination. IDC cells from 21 sections, nonmalignant IPMN cells from 28 sections, PAE cells from 20 sections, and normal pancreatic epithelial cells from 19 sections were isolated selectively with a laser microdissection and pressure catapulting system (LMPC, PALM Microlaser Technologies, Bernried, Germany) per the manufacturer's protocols. After microdissection, total RNA was extracted from the selected cells and subjected to real-time RT-PCR for quantitative measurement of *S100A6* mRNA (19). Twenty-eight samples of nonmalignant IPMN cells microdissected in the present study were divided according to the WHO classification (20) into 20 samples of adenoma and 8 samples of borderline tumor (Table 1). Recently, a consensus nomenclature and criteria have been defined for classifying variants as distinctive IPMN subtypes, including gastric type, intestinal type, pancreaticobiliary type, and oncocytic type (21). The 20 samples of adenoma comprised 19 gastric-type IPMNs and 1 intestinal-type IPMN, and the 8 samples of borderline tumor comprised 4 intestinal-type IPMNs and 4 gastric-type IPMNs (Table 1). The proportion of IPMNs with a gastric versus pancreaticobiliary or intestinal phenotype in the present study was very high compared with

Table 1. Grade and type of microdissected nonmalignant IPMNs

Type*	Adenoma †	Borderline †
Gastric	19	4
Intestinal	1	4
Pancreaticobiliary	0	0
Oncocytic	0	0

*Type was according to classification of IPMN established at the international consensus meeting held in 2003 (21).
† Grade was according to the WHO classification (20).

that reported previously (22). In the present study, we used frozen sections, which were usually taken from an area away from the center of the main tumor because the main lesions were fixed with formalin for accurate diagnosis and clinical decision making. Therefore, formalin-fixed, paraffin-embedded, and frozen sections may show significant differences due to the locations within the tumor from which they are most likely taken. In addition, in studies of formalin-fixed and paraffin-embedded samples, most dysplastic lesions are typically selected from many sections, whereas the sections from frozen samples are very limited. Therefore, the studies with formalin-fixed and paraffin-embedded samples typically contain a greater proportion of higher-grade IPMNs than studies with frozen samples. This may underlie the differences in proportion of IPMN type because pancreaticobiliary or intestinal phenotypes are often correlated with high-grade atypia. In the present study, pancreaticobiliary-type and oncocytic-type IPMNs were not included because such samples were unavailable, possibly due to the rarity of such IPMN types in Japan or because we selected nonmalignant IPMN. Representative photomicrographs of gastric-type and intestinal-type IPMNs are shown in Fig. 1.

Statistical Analyses. Data were analyzed by Kruskal-Wallis test if comparisons involved three groups and by Mann-Whitney *U* test and Spearman rank correlation test if comparisons involved two groups because normal distributions were not obtained. Statistical significance was defined as $P < 0.05$. Because we did multiple comparisons, we used Bonferroni correction; therefore, the adjusted significance levels were $P < 0.008$ for microdissection data and $P < 0.017$ for pancreatic juice data. The patient distribution was examined by χ^2 test for categorical variables and by Kruskal-Wallis test for continuous variables. The optimal cutoff points for each marker for discriminating between pancreatic carcinoma or IPMN and chronic pancreatitis were sought by constructing receiver operating characteristic (ROC) curves, which were generated by calculating the sensitivities and specificities of data for each marker at several predetermined cutoff points with the MedCalc statistical software package, version 7.6 (MedCalc, Mariakerke, Belgium; ref. 23).

Results

Quantitative Analysis of S100A6 Expression in IDC Cells, Nonmalignant IPMN Cells, PAE Cells, and Normal Epithelial Cells. In our previous study, we evaluated *S100A6* expression in normal pancreas bulk tissues and microdissected PanIN and normal ductal epithelial cells as counterparts of pancreatic cancer bulk tissues and microdissected IDC cells, respectively (5). Then, we found that pancreatic cancer bulk tissues expressed significantly higher levels of *S100A6* than did normal pancreas bulk tissues and also found that microdissected IDC, PanIN, and normal ductal cells expressed significantly different levels of *S100A6* (5).

In the clinical setting, however, it is important to distinguish pancreatic cancer from benign diseases, such as chronic pancreatitis and nonmalignant IPMN. IPMN and chronic pancreatitis samples frequently show changes in expression of tumor-related genes similar to those in pancreatic cancers (24-27). Thus, to determine whether *S100A6* is differentially expressed between pancreatic cancer, nonmalignant IPMN, and chronic pancreatitis, we did laser microdissection to isolate IDC cells, nonmalignant IPMN cells, PAE cells, and normal epithelial cells and quantified *S100A6* expression in each cell type with one-step quantitative real-time RT-PCR with gene-specific priming. As shown in Fig. 2, IDC cells and IPMN cells expressed significantly higher levels of *S100A6* than did PAE cells and normal epithelial cells (IDC or IPMN versus PAE cells or normal epithelial cells; $P < 0.0001$). IDC cells expressed higher levels of *S100A6* than did nonmalignant IPMN cells; however, this difference was not statistically significant. PAE cells expressed higher levels of *S100A6* than did normal epithelial cells, but this difference also was not statistically significant.

Nonmalignant IPMN is considered to be a precursor lesion of a subset of pancreatic cancer. It was reported that a subset of PAE cells has the potential to progress to pancreatic cancer, although this is very rare (10, 11). PanIN is also a common precursor lesion of pancreatic cancer (9). We reported previously that PanIN cells expressed higher levels of *S100A6* than did normal epithelial cells and lower levels than did IDC cells (5), which was consistent with the results of an immunohistochemical study reported by Vimalachandran et al. (6). Taken together, these data suggest that alteration of *S100A6* expression occurs at a very early stage of pancreatic carcinogenesis and that expression of *S100A6* increases in a stepwise manner during carcinogenesis.

Quantitative Analysis of *S100A6* mRNA Expression in Pancreatic Juice. The results of our microdissection-based analyses of isolated cells suggest that *S100A6* is a promising diagnostic marker to distinguish pancreatic cancer from chronic pancreatitis and nonmalignant IPMN. We analyzed *S100A6* mRNA levels in 93 pancreatic juice samples from patients with various pancreatic diseases. The baseline characteristics of the patients included in the present study are shown in Table 2. The distribution of patients did not

Gastric type Intestinal type

Figure 1. Representative photomicrographs of gastric-type and intestinal-type IPMN. H&E stain. *Inset*, lower magnification.

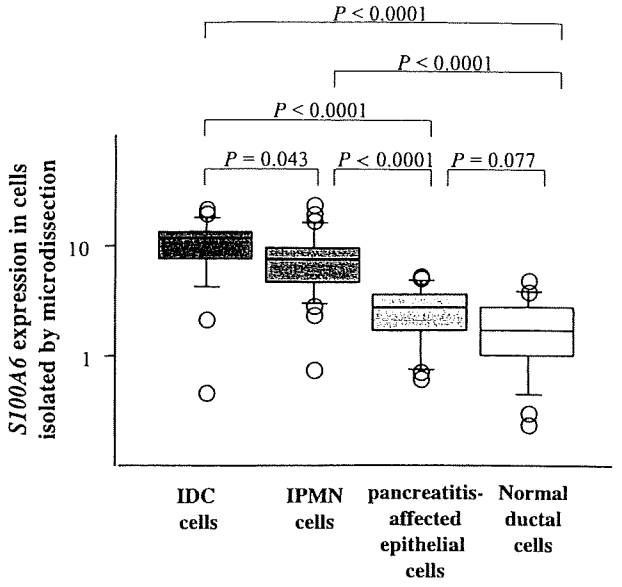

Figure 2. Microdissection-based quantitative analysis of *S100A6*. We isolated IDC cells, nonmalignant IPMN cells, PAE cells, and normal epithelial cells from frozen sections by microdissection and did one-step quantitative real-time RT-PCR with gene-specific priming to analyze expression of *S100A6* in these cells. Expression of S100A6 was normalized to that of *β-actin*. We found that IDC cells and IPMN cells express significantly higher levels of *S100A6* than do PAE cells and normal ductal epithelial cells. The median value of *S100A6* in IDC cells was higher than that in IPMN cells, although the difference was not statistically significant ($P = 0.043$). The median value of *S100A6* in PAE cells was higher than that in normal epithelial cells; however, the difference was not statistically significant ($P = 0.077$).

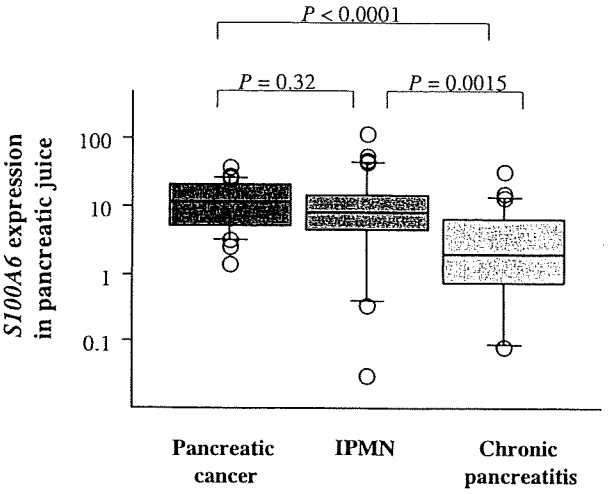

Figure 3. Quantification of *S100A6* mRNA expression in pancreatic juice. Expression of *S100A6* in pancreatic juice samples was analyzed by one-step quantitative real-time RT-PCR with gene-specific priming and short amplicons and normalized to that of *β-actin*. *S100A6* expression differed significantly between pancreatic juice from patients with cancer and those with chronic pancreatitis ($P < 0.0001$) and between pancreatic juice samples from patients with IPMN and those with chronic pancreatitis ($P = 0.0015$) after Bonferroni correction (*, $P < 0.017$). However, S100A6 expression did not differ significantly between pancreatic juice samples from patients with cancer and those with IPMN ($P = 0.32$).

differ significantly for age, sex, or comorbid conditions between patients with pancreatic cancer, nonmalignant IPMN, and chronic pancreatitis. Expression of *S100A6* was significantly higher in pancreatic cancer and IPMN samples than in chronic pancreatitis samples after Bonferroni correction ($P < 0.0001$ for pancreatic cancer versus chronic pancreatitis; $P = 0.0015$ for IPMN versus chronic pancreatitis; Fig. 3). However, *S100A6* expression did not differ significantly between pancreatic cancer and IPMN samples ($P = 0.32$; Fig. 3). To investigate *S100A6* mRNA levels in pancreatic juice from normal pancreata, we analyzed five pancreatic juice samples from patients with pancreata, which were confirmed to be normal by endoscopic retrograde cholangiopancreatography, endoscopic ultrasound, and/or computer tomography. We found that *S100A6* mRNA levels were undetectable or extremely low in pancreatic juice samples from normal pancreata compared with levels in neoplastic samples. *S100A6* mRNA levels in normal pancreatic juice were similar to those of pancreatic juice samples from pancreatitis-affected pancreata (data not shown).

Table 2. Baseline characteristics of the study population

	Pancreatic cancer	Nonmalignant IPMN*	Chronic pancreatitis	$P^{\dagger}$
Age (25%-median-75%), y	57-66-73	55-68-71	54-64.5-75	0.6
Sex (M/F ratio)	1.36	1.06	3.00	0.4
Comorbid conditions (%)				
Cardiovascular disease	19.2	22.9	17.8	0.88
Diabetes	23.1	28.5	21.4	0.79
Pulmonary disease	15.4	11.4	10.7	0.8
Cytology[‡] (%)				
I-II	53.8	90.9	100	<0.0001
III	34.6	9.1	0	
IV-V	11.5	0	0	
Stage[§] of pancreatic cancer (%)				
I-III	19.2			
IVa and IVb	80.7			
Etiology of pancreatitis (%)				
Alcoholic			42.9	
Idiopathic			32.1	
Other			25	
Relative expression of S100A6 (25%-median-75%)	5.2-11.3-21.0	4.2-8.2-14.8	0.7-1.7-4.1	<0.0001

*Intraductal papillary mucinous neoplasm.
†For continuous variables: P for Kruskal-Wallis test. For categorical variables: P for χ^2 test.
‡Cytologic classification was as described in previously (18).
§Pancreatic cancer was staged according to Japan Pancreas Society Classification (17).

As shown in Table 2, our pancreatic juice analyses included 5 (19.2%) samples from patients with stage I, II, or III pancreatic cancers and 21 (80.7%) samples from patients with stage IVa and IVb pancreatic cancers. This study also included pancreatic juice samples from patients with chronic pancreatitis with different etiologies (Table 2). However, there were no significant differences in *S100A6* expression between different stages of pancreatic cancers ($P = 0.45$) or between different etiologies of chronic pancreatitis ($P = 0.36$). In the present study, cytologic class IV or V was considered positive for a diagnosis of malignancy. The cytologic sensitivity for diagnosis of pancreatic cancer was only 11.5%, although the specificity was 100% (Table 2). The distribution of atypical grades, including class I or II, class III, and class IV or V, was significantly different between patients with pancreatic cancer, nonmalignant IPMN, and chronic pancreatitis ($P < 0.0001$; Table 2). The distribution of atypical grades was significantly different between patients with pancreatic cancer and those with chronic pancreatitis ($P = 0.0003$) and between patients with pancreatic cancer and those with nonmalignant IPMN ($P = 0.004$). However, there was no significant difference in the distribution of atypical grades between patients with nonmalignant IPMN and chronic pancreatitis ($P = 0.11$). We also examined the correlation between *S100A6* expression and cytologic evaluation and found no significant correlation ($P = 0.31$).

ROC curves for *S100A6* expressions are shown in Fig. 4. The sensitivity of the S100A6 was determined at several specificity levels. The area under the ROC curve was 0.864 for pancreatic cancer versus chronic pancreatitis [95% confidence interval (95% CI), 0.746-0.941] and 0.749 for IPMN versus chronic pancreatitis (95% CI, 0.615-0.855). The area under the ROC curve was 0.555 for pancreatic cancer versus IPMN (95% CI, 0.416-0.688). In particular, a significant difference between the areas for pancreatic cancer versus chronic pancreatitis and pancreatic cancer versus IPMN was observed (difference between areas, 0.309; 95% CI, 0.178-0.440; $P < 0.001$). These data indicate that measurements of *S100A6* mRNA levels in pancreatic juice may provide some advantage in discriminating pancreatic cancer or IPMN from chronic pancreatitis but not in discriminating pancreatic cancer from IPMN.

Discussion

In the present study, microdissection-based analyses revealed that IDC, nonmalignant IPMN, PAE, and normal epithelial cells expressed different levels of *S100A6*. Previously, we reported that IDC, PanIN, and normal epithelial cells expressed different levels of *S100A6* (5). These data suggest that expression of *S100A6* is increased in a stepwise manner during pancreatic carcinogenesis. The present pancreatic juice analyses revealed that the levels of *S100A6* in pancreatic cancer and IPMN juice samples were significantly higher than those in chronic pancreatitis-juice samples. However, the levels of *S100A6* in pancreatic juice did not differ between pancreatic cancer and IPMN juice samples, which was inconsistent with the results of the present microdissection-based analyses. Apparently, contamination of pancreatic cancer juice samples with premalignant cells could reduce *S100A6* levels measured in total cell pellets from pancreatic juice samples. Thus, to examine the true levels of *S100A6* in highly dysplastic cells in pancreatic juice samples, microdissection of cell pellets from pancreatic juice samples is needed. Such studies are presently under way in our laboratory.

Several pancreatic juice markers, including *k-ras* mutations, telomerase activity, and *hTERT* mRNA, have been reported (16, 28, 29). Recently, mutations of *k-ras* in pancreatitis-affected pancreata and pancreatic cancer were reported (30). Because *k-ras* mutation analysis is qualitative, it may be difficult to monitor the progression of carcinogenesis, whereas the present *S100A6* mRNA analysis is quantitative. We reported previously that quantitative analysis of telomerase activity is useful for differentiation of pancreatic cancer from nonmalignant IPMN or chronic pancreatitis (16, 29). However, there is no way to check sample quality for telomerase activity assays; therefore, it is difficult to use this assay in routine clinical settings. We also reported that quantitative analysis of *hTERT* mRNA, which is a subunit of telomerase, is useful for distinguishing pancreatic cancer from nonmalignant IPMN (31). Although we can easily check the quality of RNAs, our results suggested that *hTERT* analysis is not useful for distinguishing pancreatic cancer from chronic pancreatitis because relatively high levels of *hTERT* mRNA are expressed by activated lymphocytes in chronic pancreatitis-related pancreatic juice. In the present study, we found that pancreatic cancer and nonmalignant IPMN expressed significantly higher levels of *S100A6* than did chronic pancreatitis-related pancreatic juice samples. Apparently, activation of telomerase or overexpression of *hTERT* mRNA occurs at a later stage of pancreatic carcinogenesis, whereas overexpression of *S100A6* may occur at an early stage of pancreatic carcinogenesis and may increase in a stepwise manner during the progression of pancreatic carcinogenesis. Therefore, compared with telomerase activity and *hTERT* mRNA assays, quantitative analysis of *S100A6* is especially useful for monitoring the progression of carcinogenesis in individuals with high risk of pancreatic cancer, such as those with a familial history or chronic pancreatitis, or for screening individuals with high-risk lesions that may progress to pancreatic cancer.

To date, no single biomarker has been proven to have sufficient diagnostic accuracy to serve as a stand-alone means for early detection and diagnosis of cancer. Thus, biomarkers can be of significant clinical value by providing evidence to

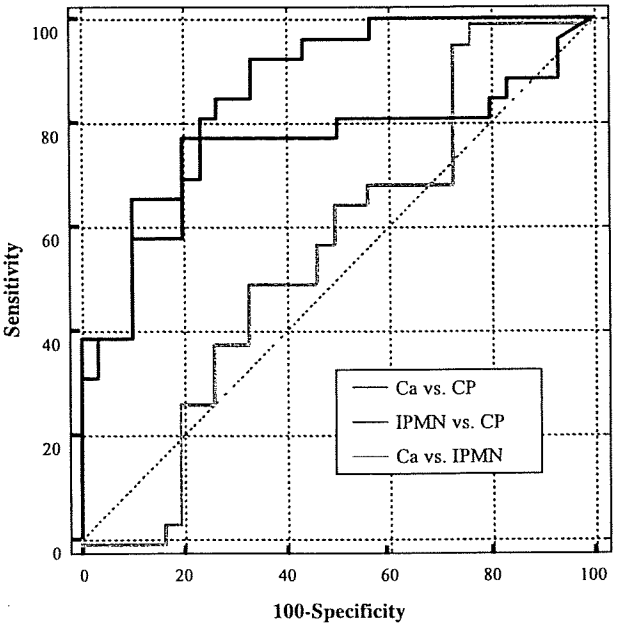

Figure 4. ROC curve analyses of S100A6 expression in pancreatic juice samples. Sensitivity of *S100A6* analysis was determined at several specificity levels. The areas under the ROC curve were 0.864 for pancreatic cancer versus chronic pancreatitis (95% CI, 0.746-0.941) and 0.749 for IPMN versus chronic pancreatitis (95% CI, 0.615-0.855). The area under the ROC curve was 0.555 for pancreatic cancer versus IPMN (95% CI, 0.416-0.688). The results of ROC curve analyses suggest that *S100A6* expression status can be used to differentiate pancreatic cancer or IPMN from chronic pancreatitis. *Ca*, pancreatic cancer; *CP*, chronic pancreatitis.

suspect cancer or, when combined with other clinical data, to aid in differential diagnosis. In the present study, the *S100A6* analyses of pancreatic juice yielded statistically significant differences between neoplastic samples, such as pancreatic cancer and nonmalignant IPMN and chronic pancreatitis samples, and our microdissection analyses revealed that expression of *S100A6* is increased in a stepwise manner during pancreatic carcinogenesis. Therefore, *S100A6* analysis of pancreatic juice may aid in differential diagnosis if combined with other clinical data and may have some advantages to detect or screen for pancreatic cancer and to follow up with individuals with high-risk factors, such as familial pancreatic cancer.

Acknowledgments

We thank M. Ohta (Department of Clinical Pathology, Kyushu University) for skillful cytologic examination and analysis.

References

1. Jemal A, Murray T, Samuels A, Ghafoor A, Ward E, Thun MJ. Cancer statistics, 2003. CA Cancer J Clin 2003;53:5–26.
2. Taylor B. Carcinoma of the head of the pancreas versus chronic pancreatitis: diagnostic dilemma with significant consequences. World J Surg 2003;27: 1249–57.
3. Ohhashi K, Murakami F, Maruyama M, et al. Four cases of mucous secreting pancreatic cancer [in Japanese with English abstract]. Prog Dig Endosc 1982; 203:348–351.
4. Yamaguchi K, Ohuchida J, Ohtsuka T, Nakano K, Tanaka M. Intraductal papillary-mucinous tumor of the pancreas concomitant with ductal carcinoma of the pancreas. Pancreatology 2002;2:484–90.
5. Ohuchida K, Mizumoto K, Ishikawa N, et al. The role of S100A6 in pancreatic cancer development and its clinical implication as a diagnostic marker and therapeutic target. Clin Cancer Res 2005;11:7785–93.
6. Vimalachandran D, Greenhalf W, Thompson C, et al. High nuclear S100A6 (calcyclin) is significantly associated with poor survival in pancreatic cancer patients. Cancer Res 2005;65:3218–25.
7. Logsdon CD, Simeone DM, Binkley C, et al. Molecular profiling of pancreatic adenocarcinoma and chronic pancreatitis identifies multiple genes differentially regulated in pancreatic cancer. Cancer Res 2003;63: 2649–57.
8. Breen EC, Tang K. Calcyclin (S100A6) regulates pulmonary fibroblast proliferation, morphology, and cytoskeletal organization *in vitro*. J Cell Biochem 2003;88:848–54.
9. Hruban RH, Adsay NV, Albores-Saavedra J, et al. Pancreatic intraepithelial neoplasia: a new nomenclature and classification system for pancreatic duct lesions. Am J Surg Pathol 2001;25:579–86.
10. Lowenfels AB, Maisonneuve P, Cavallini G, et al. Pancreatitis and the risk of pancreatic cancer. International Pancreatitis Study Group. N Engl J Med 1993;328:1433–7.
11. Karlson BM, Ekbom A, Josefsson S, McLaughlin JK, Fraumeni JF, Jr., Nyren O. The risk of pancreatic cancer following pancreatitis: an association due to confounding? Gastroenterology 1997;113:587–92.
12. Antonov J, Goldstein DR, Oberli A, et al. Reliable gene expression measurements from degraded RNA by quantitative real-time PCR depend on short amplicons and a proper normalization. Lab Invest 2005;85:1040–50.
13. Lekanne Deprez RH, Fijnvandraat AC, Ruijter JM, Moorman AF. Sensitivity and accuracy of quantitative real-time polymerase chain reaction using SYBR Green I depends on cDNA synthesis conditions. Anal Biochem 2002; 307:63–9.
14. Lewis F, Maughan NJ, Smith V, Hillan K, Quirke P. Unlocking the archive—gene expression in paraffin-embedded tissue. J Pathol 2001;195:66–71.
15. Ohuchida K, Mizumoto K, Yamada D, et al. Quantitative analysis of MUC1 and MUC5AC mRNA in pancreatic juice for preoperative diagnosis of pancreatic cancer. Int J Cancer 2006;118:405–11.
16. Ohuchida K, Mizumoto K, Ogura Y, et al. Quantitative assessment of telomerase activity and human telomerase reverse transcriptase messenger RNA levels in pancreatic juice samples for the diagnosis of pancreatic cancer. Clin Cancer Res 2005;11:2285–92.
17. Japan Pancreas Society. Classification of pancreatic carcinoma. Second English Edition. Tokyo: Kanehara & Co., Ltd.; 2003.
18. Yamaguchi K, Nakamura M, Shirahane K, et al. Pancreatic juice cytology in IPMN of the pancreas. Pancreatology 2005;5:416–21; discussion 21.
19. Tachikawa T, Irie T. A new molecular biology approach in morphology: basic method and application of laser microdissection. Med Electron Microsc 2004;37:82–8.
20. World Health Organization classification of tumors: pathology and genetics of tumors of the digestive system. Lyon: IARC Press; 2000.
21. Furukawa T, Kloppel G, Volkan Adsay N, et al. Classification of types of intraductal papillary-mucinous neoplasm of the pancreas: a consensus study. Virchows Arch 2005;447:794–9.
22. Adsay NV, Merati K, Basturk O, et al. Pathologically and biologically distinct types of epithelium in intraductal papillary mucinous neoplasms: delineation of an "intestinal" pathway of carcinogenesis in the pancreas. Am J Surg Pathol 2004;28:839–48.
23. Zweig MH, Campbell G. Receiver-operating characteristic (ROC) plots: a fundamental evaluation tool in clinical medicine. Clin Chem 1993;39: 561–77.
24. Biankin AV, Biankin SA, Kench JG, et al. Aberrant p16(INK4A) and DPC4/Smad4 expression in intraductal papillary mucinous tumours of the pancreas is associated with invasive ductal adenocarcinoma. Gut 2002;50: 861–8.
25. Soldini D, Gugger M, Burckhardt E, Kappeler A, Laissue JA, Mazzucchelli L. Progressive genomic alterations in intraductal papillary mucinous tumours of the pancreas and morphologically similar lesions of the pancreatic ducts. J Pathol 2003;199:453–61.
26. Hermanova M, Nenutil R, Kren L, Feit J, Pavlovsky Z, Dite P. Proliferative activity in pancreatic intraepithelial neoplasias of chronic pancreatitis resection specimens: detection of a high-risk lesion. Neoplasma 2004;51: 400–4.
27. Rosty C, Geradts J, Sato N, et al. p16 Inactivation in pancreatic intraepithelial neoplasias (PanINs) arising in patients with chronic pancreatitis. Am J Surg Pathol 2003;27:1495–501.
28. Tada M, Omata M, Kawai S, et al. Detection of ras gene mutations in pancreatic juice and peripheral blood of patients with pancreatic adenocarcinoma. Cancer Res 1993;53:2472–4.
29. Ohuchida K, Mizumoto K, Ishikawa N, et al. A highly sensitive and quantitative telomerase activity assay with pancreatic juice is useful for diagnosis of pancreatic carcinoma without problems due to polymerase chain reaction inhibitors: analysis of 100 samples of pancreatic juice from consecutive patients. Cancer 2004;101:2309–17.
30. Tada M, Ohashi M, Shiratori Y, et al. Analysis of K-ras gene mutation in hyperplastic duct cells of the pancreas without pancreatic disease. Gastroenterology 1996;110:227–31.
31. Ohuchida K, Mizumoto K, Yamada D, et al. Quantitative analysis of human telomerase reverse transcriptase in pancreatic cancer. Clin Cancer Res 2006; 12:2066–9.

ANTICANCER RESEARCH 27: 793-800 (2007)

Increased Expression of *ADAM 9* and *ADAM 15* mRNA in Pancreatic Cancer

DAISUKE YAMADA, KENOKI OHUCHIDA, KAZUHIRO MIZUMOTO, SEIJI OHHASHI, JUN YU, TAKUYA EGAMI, HAYATO FUJITA, EISHI NAGAI and MASAO TANAKA

Department of Surgery and Oncology, Graduate School of Medical Sciences, Kyushu University, Fukuoka, Japan

Abstract. *Background: A disintegrin and metalloproteases (ADAMs) comprise a multifunctional family of membrane-anchored proteins. ADAM 9 and ADAM 15 are involved in cell migration and invasion. Expression of ADAM 9 and ADAM 15 was reported to be altered in several types of cancer. Materials and Methods: Quantitative real-time reverse transcription-polymerase chain reaction was performed to measure the expression of ADAM 9 mRNA in bulk pancreatic tissues. Results showed no significant difference in the expression of ADAM 9 mRNA between pancreatic cancer and non-neoplastic pancreas. Primary cultured pancreatic fibroblasts also expressed ADAM 9 mRNA. Therefore, a laser microdissection and pressure catapulting technique was employed to isolate cancer cells from tumor tissues. The expression of ADAM 9 and ADAM 15 mRNA was measured in microdissected samples (cancer cells, n=11; normal epithelial cells, n=13 for ADAM 9; cancer cells, n=9; normal epithelial cells, n=9 for ADAM 15). Results: Pancreatic cancer cells expressed significantly higher levels of ADAM 9 and ADAM 15 mRNA than did normal pancreatic epithelial cells (p=0.016 for ADAM 9; p=0.004 for ADAM 15). Conclusion: ADAM 9 and ADAM 15 are involved in pancreatic cancer. Microdissection-based analysis appears to be indispensable for the accurate analysis of the expression of certain ADAM family members in pancreatic cancer.*

Pancreatic cancer is one of the most lethal cancers with an overall 5-year survival rate after resection of approximately 10-20% (1). Despite improvements in chemotherapy and radiotherapy, the prognosis for pancreatic cancer has remained poor for decades because of its extremely aggressive nature. In order to improve the prognosis for pancreatic cancer, the identification of novel target genes for therapy is necessary.

Approximately 40 members have been identified of the family of multifunctional membrane-anchored proteins known as ADAMs (a disintegrin and metalloproteases). ADAMs are composed of a metalloprotease, a disintegrin, a cysteine-rich, an epidermal growth factor (EGF)-like, a transmembrane and a cytoplasmic domain (2). Each domain exerts its own unique functions. The metalloprotease domain cleaves the ectodomains of cytokines, growth factors, receptors and other molecules. The disintegrin domain binds integrins and is involved in cell-cell and cell-matrix interactions (3). Each ADAM exerts diverse functions according to the targets of the metalloprotease domain and the binding sites of the disintegrin domain.

ADAM 9 has been reported to be overexpressed in several cancers (4-9). Targets of the ADAM 9 metalloprotease domain are epidermal growth factor receptor (EGFR) ligands (10), and the disintegrin domain of ADAM 9 binds alfa(v)beta(5) (11), alfa(9)beta(1) (12) and alfa(6)beta(1) (13) integrins and degrades extracellular matrix (ECM) components including fibronectin and gelatin (12). On the basis of these functions, ADAM 9 is believed to be involved in malignancy. Many recent studies have suggested a relation between ADAM 9 and various cancers. ADAM 9 has been reported to be up-regulated in breast (4, 5) and prostate cancer (6) and has been associated with tumor aggressiveness and progression in liver (7) and non-small cell lung cancer (9). Gene expression profiling by microarray has suggested that *ADAM 9* is overexpressed in pancreatic cancer and its cell lines (14, 15). Immunohistochemistry has also suggested that ADAM 9 expression is associated with poor tumor differentiation and poor patient prognosis in pancreatic cancer (16).

ADAM15 has been reported to be dysregulated in several cancers (17-19). Targets of the ADAM 15 metalloprotease domain include amphiregulin, epiregulin (20) and CD23 (21). Amphiregulin and epiregulin constitute EGFR ligands. The disintegrin domain of ADAM 15 binds alfa(5)beta(1)

Correspondence to: Dr. K. Mizumoto, Department of Surgery and Oncology, Graduate School of Medical Sciences, Kyushu University, 3-1-1 Maidashi, Fukuoka 812-8582, Japan. Tel: +81 92 642 5440, Fax: +81 92 642 5458, e-mail: mizumoto@med.kyushu-u.ac.jp

Key Words: ADAM 9, ADAM 15, pancreatic cancer, microdissection, quantitative real-time RT-PCR.

0250-7005/2007 $2.00+.40

(22), alfa(v)beta(3) (23) and alfa(9)beta(1) (24) integrins and degrades ECM components including Type IV collagen and gelatin (12). On the basis of these functions, *ADAM 15* is also thought to be involved in malignancy. ADAM 15 and ADAM 9 have been shown to be up-regulated in gastric cancer (17). ADAM 15 expression has also been reported to be associated with aggressive prostate and breast cancers (18). Schutz *et al.* (19) reported that ADAM 15 was frequently detected in lung carcinoma cell lines and tissues, and that lung cancer cells located at the invasion front expressed significantly higher levels of ADAM 15 than those located within the tumor center. To date, however, there have been no reports regarding the expression of ADAM 15 in pancreatic cancer.

In the present study, to clarify the involvement of ADAM 9 and ADAM 15 in pancreatic cancer, we investigated mRNA expression using one-step quantitative real-time reverse transcriptase-polymerase chain reaction (real-time RT-PCR).

Materials and Methods

Cultured cells and pancreatic tissues. The following 13 human pancreatic cancer cell lines were used: ASPC-1, BxPC-3, KP-1N, KP-2, Panc-1 and SUIT-2 (Dr. H. Iguchi, National Kyushu Cancer Center, Fukuoka, Japan); MIA PaCa-2 (Japanese Cancer Resource Bank, Tokyo, Japan); Capan-1, Capan-2, CFPAC-1, SW1990 and HS766T (American Type Culture Collection, Manassas, VA, USA), and NOR-P1 (established from a metastatic subcutaneous tumor of a patient with pancreatic cancer; 25). Six primary cultures of pancreatic fibroblasts derived from patients with invasive pancreatic adenocarcinoma were used in the present study. Cells were maintained as described elsewhere (26). Tissue samples were obtained during surgery at Kyushu University Hospital (Fukuoka, Japan) during the period February 15, 2001 to July 15, 2005, as described elsewhere (27). A total of 23 pancreatic cancer tissue samples were obtained from the primary tumor of each resected pancreas. The diagnosis of pancreatic cancer was confirmed by histological examination of resected specimens. Twelve non-neoplastic pancreata were obtained away from the pancreatic tumor or were normal pancreata resected due to cholangiocarcinoma, as described elsewhere (27). Experienced pathologists performed histological examination of all tissues adjacent to the specimens. Written informed consent was obtained from all patients and the study was approved by our institution's surveillance committee and conducted according to the Helsinki Declaration.

Isolation of total RNA. Total RNA was extracted according to the standard acid guanidinium thiocyanate phenol chloroform protocol (28), with glycogen (Funakoshi, Tokyo, Japan). Pancreatic cancer cells and normal pancreatic epithelial cells were isolated from frozen sections using a laser microdissection and pressure catapulting system (LMPC) and then extracted total RNA from these isolated cells. RNA extracts were measured with a NanoDrop ND-1000 spectrophotometer (NanoDrop Technologies, Inc., Rockland, DE, USA), at 260 nm and 280 nm. RNA integrity was assessed with an Agilent Bioanalyzer 2100 (Agilent Technologies, Palo Alto, CA, USA).

Quantitative analysis of ADAM 9 and ADAM 15 mRNA levels via one-step real-time RT-PCR with gene-specific primers. One-step quantitative real-time RT-PCR was used with gene-specific primers to examine mRNA levels of *ADAM 9* and *ADAM 15*. We designed specific primers (ADAM 9 forward: 5'-gttcctgtggagcaaagagc-3', reverse: 5'-ccagcgtccaccaacttatt-3'; ADAM 15 forward: 5'-agcctcaaaaaggtgcttca-3', reverse: 5'-ccctggtagcagcagttctc-3'; 185 rRNA forward: 5'-ccatccaatcggtagtagcg-3', reverse: 5'-gtaacccgttgaaccccatt-3') BLAST searches to ensure the specificity of these primers. One-step quantitative real-time RT-PCR with gene-specific primers was performed with a QuantiTect SYBR Green RT-PCR Kit (Qiagen K.K., Tokyo, Japan) and a LightCycler Quick System 350S (Roche Diagnostics K.K., Tokyo, Japan). The reaction mixture was incubated at 50°C for 20 min to allow for reverse transcription, during which first-strand cDNA was synthesized by priming with a gene-specific primer. PCR was initiated with one cycle of 95°C for 15 min to activate modified Taq polymerase followed by 40 cycles of 94°C for 15 sec, 55°C for 25 sec and 72°C for 10 sec, followed by one cycle of 95°C for 0 sec, 65°C for 15 sec and +0.1°C/s to 95°C for melting analysis to visualize nonspecific PCR products, different fragments showed separate distinct melting peaks. Each primer set used in the present study produced a single melting peak and a single prominent band of expected size on microchip electrophoresis. Each sample was run twice and any sample showing greater than 10% deviation from the RT-PCR value was tested a third time. Levels of mRNA in each sample were calculated from a standard curve generated with total RNA from Capan-1 human pancreatic cancer cells. Levels of *ADAM 9* and *ADAM 15* mRNA were normalized to that of *18S rRNA*. Samples were used that showed ADAM levels greater than the levels of *18S rRNA* corresponding to 0.05 ng of total RNA derived from Capan-1 cells. When levels of *ADAM 9* or *ADAM 15* mRNA were not detected due to the limitation of our real-time RT-PCR-based assay (the level corresponding to 0.01 ng of total RNA derived from Capan-1 cells), expression values were defined as this level.

Microdissection-based quantitative analysis of ADAM 9 and ADAM 15 mRNA. Frozen tissue samples were cut into 8-μm-thick sections. One section was stained with hematoxylin and eosin (H&E) for histological examination. We used a laser microdissection and pressure catapulting system (LMPC; PALM MicroLaser Technologies AG, Bernried, Germany), according to the manufacturer's instructions to selectively isolate pancreatic cancer cells from 11 sections and normal pancreatic epithelial cells from 13 sections for quantification of *ADAM 9* mRNA, and pancreatic cancer cells from 9 sections and normal pancreatic epithelial cells from 9 sections for quantification of *ADAM 15* mRNA. After microdissection, total RNA was extracted from the isolated cells and was subjected to one-step real-time RT-PCR for quantitative measurement of *ADAM 9* or *ADAM 15* mRNA.

Statistical analysis. Data were analyzed using the Mann-Whitney *U*-test because the data did not follow a normal distribution. Statistical significance was set at $p<0.05$.

Results

Quantitative analysis of ADAM 9 mRNA expression in bulk tissues of pancreatic cancer and non-neoplastic pancreas. ADAM 9 mRNA expression did not differ significantly between bulk tissues of pancreatic cancer and non-